

RESEARCH MEMORANDUM

FLIGHT MEASUREMENTS WITH THE DOUGLAS D-558-II

(BUAERO NO. 37974) RESEARCH AIRPLANE

STATIC LONGITUDINAL STABILITY AND CONTROL CHARACTERISTICS

AT MACH NUMBERS UP TO 0.87

By S. A. Sjoberg, James R. Peele,
and John H. Griffith

Langley Aeronautical Laboratory
Langley Field, Va.

**NATIONAL ADVISORY COMMITTEE
FOR AERONAUTICS**

WASHINGTON

January 17, 1951
Declassified May 8, 1957

NATIONAL ADVISORY COMMITTEE FOR AERONAUTICS

RESEARCH MEMORANDUM

FLIGHT MEASUREMENTS WITH THE DOUGLAS D-558-II

(BUAERO NO. 37974) RESEARCH AIRPLANE

STATIC LONGITUDINAL STABILITY AND CONTROL CHARACTERISTICS

AT MACH NUMBERS UP TO 0.87

By S. A. Sjoberg, James R. Peele,
and John H. Griffith

SUMMARY

Flight measurements were made with the Douglas D-558-II research airplane to determine the longitudinal stability and control characteristics in both steady flight and accelerated flight.

With the slats locked and the flaps up the airplane was longitudinally unstable at normal-force coefficients greater than approximately 0.8 in steady flight at low speeds and in maneuvering flight at Mach numbers up to at least 0.65. No data were obtained at high normal-force coefficients at Mach numbers greater than about 0.65 because of the power limitations of the airplane with only the jet engine installed. The instability proved objectionable to the pilots particularly in accelerated flight because of the tendency for the airplane to pitch to high angles of attack very rapidly and because violent rolling and yawing motions sometimes occurred when the high angles of attack were reached. The instability probably resulted from a large increase in the rate of change of effective downwash at the tail with increase in angle of attack at moderate and high angles of attack.

With the flaps down and the slats locked, the longitudinal stability characteristics in steady flight at low speeds were very similar to the characteristics with the flaps up and the slats locked, except that the instability occurred at a higher normal-force coefficient.

The degree of instability present with the slats unlocked and the flaps up or down was much less than with the slats locked and the pilots had only minor objections to the longitudinal characteristics of the airplane.

In steady flight in the Mach number range from 0.50 to 0.87 the airplane was stable longitudinally and no abrupt trim changes occurred up to the highest Mach number reached, 0.87. The data indicate that only a slight reduction in the relative elevator-stabilizer effectiveness occurred in going from a Mach number of about 0.55 to 0.85.

In turning flight at low lift coefficients the values of $d\delta_e/dC_{NA}$ and $\Delta F_e/\Delta g$ were approximately doubled as the Mach number was increased from 0.6 to 0.87. Most of the increase in $d\delta_e/dC_{NA}$ and $\Delta F_e/\Delta g$ can be attributed to an increase in the stability of the airplane which occurred because of the increase in the stability of the wing-fuselage combination. At a Mach number of 0.4 the aerodynamic center of the wing-fuselage combination is at about 10 percent of the mean aerodynamic chord, and at a Mach number of 0.87 the aerodynamic center is at about 20 percent of the mean aerodynamic chord.

INTRODUCTION

As a part of the cooperative Navy-NACA Transonic Flight Research Program the NACA is utilizing the Douglas D-558-II (BuAero No. 37974) research airplane. These tests are being made at the NACA High-Speed Flight Research Station at Edwards Air Force Base, Calif. This paper presents measurements of the longitudinal stability and control characteristics in both steady flight and accelerated flight. Data are presented for a speed range from the stalling speed up to a maximum Mach number of 0.87.

References 1 to 7 present flight measurements of other aerodynamic characteristics of the Douglas D-558-II airplane. Reference 7 presents flight measurements of the pitching-moment characteristics of the wing and the wing-fuselage combination; therefore, correlation between the longitudinal flying qualities reported herein and the pitching-moment characteristics of the wing-fuselage combination can be obtained by referring to reference 7.

COEFFICIENTS AND SYMBOLS

δ_e	elevator deflection with respect to stabilizer, degrees
δ_{aT}	total aileron deflection, degrees
δ_r	rudder deflection, degrees

i_T	stabilizer setting with respect to fuselage center line, positive when leading edge of stabilizer is up, degrees
d_s	slat position, inches (see fig. 4)
F_e	elevator control force, pounds
F_a	aileron control force, pounds
F_r	rudder control force, pounds
n	normal acceleration, g
g	acceleration due to gravity
a_y	lateral acceleration, g
C_{N_A}	airplane normal-force coefficient (nW/qS)
W	airplane weight, pounds
q	free-stream dynamic pressure, pounds per square foot
S	wing area, square feet
C_{N_T}	horizontal-tail normal-force coefficient, positive for up tail load (L_T/qS_T)
L_T	aerodynamic load acting on horizontal tail, pounds
S_T	horizontal-tail area, square feet
M	free-stream Mach number
H_p	pressure altitude, feet
V_c	calibrated airspeed, miles per hour
α	angle of attack of airplane center line, degrees
p	rolling velocity, radians per second
r	yawing velocity, radians per second
q'	pitching velocity, radians per second

$\frac{d\delta_e}{dC_{N_A}}$	rate of change of elevator deflection required for trim with change in airplane normal-force coefficient, degrees
$\frac{\Delta F_e}{\Delta g}$	elevator control force per g of acceleration, pounds per g
a.c. _{WF}	aerodynamic-center location of wing-fuselage combination, percent mean aerodynamic chord
$\frac{\Delta\alpha_T}{\Delta\delta_e}$	relative elevator-stabilizer effectiveness

AIRPLANE

The Douglas D-558-II airplanes have sweptback wing and tail surfaces and were designed for combination turbojet and rocket power. The airplane used in the present investigation (BuAero No. 37974) does not yet have the rocket engine installed. This airplane is powered solely by a J-34-WE-40 turbojet engine which exhausts out of the bottom of the fuselage between the wing and the tail. Photographs of the airplane are shown in figures 1 and 2 and a three-view drawing is shown in figure 3. Pertinent airplane dimensions and characteristics are listed in table I.

Both slats and fences are incorporated on the wing of the airplane. The wing slats can be locked in the closed position or they can be unlocked. When the slats are unlocked the slat position is a function of the angle of attack of the airplane. Also, the slats on the left and right wings are interconnected and therefore, at any time, have the same position. Figure 4 is a drawing of the wing section showing the wing slat in the closed and extended positions.

The airplane is equipped with an adjustable stabilizer but no means are provided for trimming out aileron or rudder control forces. No aerodynamic balance or control-force booster system is used on any of the controls. Hydraulic dampers are installed on all control surfaces to aid in preventing any control-surface flutter. Dive brakes are located on the rear portion of the fuselage.

Figure 5 shows the variation of elevator position with control wheel position. The friction in the elevator control system as measured on the ground under no load is presented in figure 6. The friction measurements were obtained by measuring the control position and control force as the control was deflected slowly. The rate of control-surface

deflection during the friction measurements was sufficiently low so that the control forces resulting from the hydraulic dampers in the control system were negligible.

INSTRUMENTATION

Standard NACA recording instruments were installed in the airplane to measure the following quantities:

- Airspeed
- Altitude
- Elevator and aileron wheel forces
- Rudder pedal force
- Normal, longitudinal, and lateral accelerations
- Rolling, pitching, and yawing velocities
- Angle of attack
- Stabilizer, elevator, rudder, left and right aileron positions and slat position

Strain gages were installed on the airplane structure to measure wing and tail loads. The outputs of the strain gages were recorded on an 18-channel recording oscillograph. The strain gages were calibrated in terms of tail load by applying known loads at many points on the tail structure. The measured outputs of the gages were utilized to obtain equations from which the load on the tail could be found from the gage responses during flight. In flight, the strain gages respond to a combination of aerodynamic and inertia loads. The tail loads given in this paper have been corrected for inertia effects and therefore represent the aerodynamic loads.

The aileron positions were measured on bell cranks about 1 foot forward of the ailerons. The rudder and stabilizer positions were measured on the control surfaces. In some cases the elevator position was measured on the elevator actuating arm in the fuselage and in other cases the elevator position was measured on the surface. The elevator positions presented were measured with respect to the stabilizer and the stabilizer position was measured with respect to the fuselage center line. All control positions were measured perpendicular to the control hinge line. The slat position as used in this paper is defined in figure 4 by the distance d_s .

A free-swiveling airspeed head was used to measure both static and total pressures. The airspeed head was mounted on a boom 7 feet forward of the nose of the airplane. A vane, which was used to measure angle of attack, was mounted below the same boom $4\frac{1}{2}$ feet forward of the nose of the airplane. (See fig. 1.)

The calibration of the airspeed installation was accomplished in the Mach number range from 0.30 to 0.70 by making tower passes. The details of the tower-pass method of obtaining airspeed calibrations are given in reference 8. In order to extend the calibration up to a Mach number of 0.90 the following procedure was used. The blocking error due to the fuselage was assumed to be constant. For the combination of fuselage shape and airspeed boom length used, this assumption is justified on the basis of results reported in reference 9. The blocking error due to the airspeed head was established up to a Mach number of 0.85 from wind-tunnel tests. By combining the constant blocking error of the fuselage with the blocking error due to the airspeed head the airspeed calibration was extended up to a Mach number of 0.85. For Mach numbers greater than 0.85 and less than 0.30 the calibration was extrapolated. Also, at any given Mach number the same correction was applied at all angles of attack.

The angle-of-attack vane was not calibrated for position error in flight. Since the angle-of-attack vane was far forward of the wing of the airplane (about 1.6 wing semispans) the position error of the vane would be expected to be small. The error in the measured angles of attack resulting from boom bending was determined experimentally and the angle-of-attack measurements presented in this paper have been corrected for boom bending.

TESTS, RESULTS, AND DISCUSSION

The static longitudinal stability and control characteristics of the Douglas D-558-II airplane were determined both in steady (1 g) flight and in accelerated flight for a speed range from the stalling speed up to a maximum Mach number of 0.87. The data were obtained in the altitude range from 12,000 to 25,000 feet and the airplane's center-of-gravity location during the investigation was in the range from 26.1 to 27.4 percent of the wing mean aerodynamic chord.

Longitudinal Characteristics in Steady Flight

Low speeds.- The static longitudinal stability characteristics in steady flight at low speeds were determined for four different airplane configurations:

- (1) Flaps up, landing gear up, slats locked
- (2) Flaps up, landing gear up, slats unlocked

- (3) Flaps down, landing gear down, slats locked
- (4) Flaps down, landing gear down, slats unlocked

The data were obtained by taking continuous records as the speed was reduced from a speed 30 to 90 miles per hour above the stalling speed down to the stalling speed. During these tests the jet engine was set at idle thrust.

The data for the airplane in the flaps-up, landing-gear-up, slats-locked configuration are presented in figure 7. Figure 7(a) shows the variation of elevator position, elevator control force, tail normal-force coefficient, and angle of attack with indicated airspeed and figure 7(b) shows the variation of elevator position, tail normal-force coefficient, and airplane normal-force coefficient with angle of attack. Inspection of figure 7(a) shows that the airplane was stable longitudinally in the speed range from 230 to 165 miles per hour as shown by the increasing up-elevator deflections and increasing pull forces required for trim with decrease in airspeed. At an indicated airspeed of about 165 miles per hour the airplane became longitudinally unstable and was unstable down to the lowest speed reached, 148 miles per hour. Figure 7(b) indicates that the longitudinal instability occurred at an angle of attack of about 9° or a normal-force coefficient of about 0.80. When the airplane was unstable the pilots experienced difficulty in balancing or trimming the airplane. Therefore, the data presented for the speed and angle-of-attack range in which the airplane was unstable only approximately represent the quantities required for trim and balance. The tail normal-force-coefficient data of figure 7(b) show that for angles of attack less than about 9° where the airplane was stable the wing-fuselage combination was destabilizing since the tail normal-force coefficient required for balance increased positively with increase in angle of attack or increase in airplane normal-force coefficient. However, for angles of attack of 11° to 13.5° where the airplane was unstable the wing-fuselage combination was stabilizing since the tail normal-force coefficient required for balance decreased as the angle of attack and airplane normal-force coefficient increased. For angles of attack greater than approximately 13.5° the wing-fuselage combination was again destabilizing. These results are in agreement with data presented in reference 10 which reports results of a wind-tunnel investigation made in the Southern California Cooperative Wind Tunnel with a model of the Douglas D-558-II airplane. Further information on the stability characteristics of the wing and the wing-fuselage combination are reported in reference 7.

The data, therefore, indicate that the instability of the airplane at angles of attack greater than 9° was not due to a destabilizing effect from the wing-fuselage combination. The instability probably resulted from an increase in the rate of change of the effective downwash at the tail with change in angle of attack at the higher angles of

attack. Data presented in reference 11 for a wing having 42° of sweep-back show that, for horizontal-tail positions relatively high above the wing chord plane, as is the case with the Douglas D-558-II airplane (the horizontal tail is about 0.4 wing semispans above the wing chord plane), a large increase in the rate of change of effective downwash with change in angle of attack occurs at moderate and high angles of attack. The data of reference 11 also show that, for horizontal-tail positions below the chord plane, a decrease in the rate of change of the effective downwash with angle of attack occurs at high angles of attack.

The pilots reported that when flying in the angle-of-attack range for which the airplane was unstable it was extremely difficult to maintain the airplane at a reasonably constant speed or attitude. However, in the pilot's opinion and as will be shown later in this paper, the instability was not nearly as objectionable to the pilot when it occurred in 1 g flight as when it occurred in accelerated maneuvers.

The data for the flaps-up, landing-gear-up, slats-unlocked airplane configuration are presented in figures 8(a) and 8(b). In this airplane configuration the airplane was longitudinally stable at indicated airspeeds greater than 155 to 160 miles per hour. At airspeeds between 155 and 140 miles per hour the airplane was unstable, but the degree of instability was not nearly so great as with the slats locked (fig. 7). At indicated airspeeds less than 140 miles per hour the data presented in figure 8(a) indicate the airplane is very stable longitudinally. However, from the data of figure 8(b) showing the variation of the elevator deflection required for balance with angle of attack the airplane appears to be neutrally stable or slightly unstable in the angle-of-attack range from 22° to 28° . Also from figure 8(b) at angles of attack of 18° to 37° the tail normal-force-coefficient data show that the wing-fuselage combination again becomes destabilizing. Again the data at the high angles of attack only indicate the trends and are not the absolute quantities required for trim or balance. The data indicate that with the slats unlocked the instability occurred at a somewhat higher angle of attack and airplane normal-force coefficient than with the slats locked, the angle of attack and airplane normal-force coefficient for instability being about 11° and 0.90 with the slats unlocked and 9° and 0.80 with the slats locked. The variation of the slat position with angle of attack was smooth and the slats were fully open for angles of attack greater than 10.5° .

The pilots had only minor objections to the instability which was present in the speed range from 140 to 155 miles per hour and the instability at the high angles of attack (22° to 28°). Uncontrolled-rolling and yawing motions due to stalling were present when the airplane was unstable in the high angle-of-attack range. These motions were much more noticeable to the pilot than the longitudinal instability.

Presented in figures 9(a) and 9(b) are the data for the flaps-down, landing-gear-down, slats-locked configuration. In this configuration the airplane was stable at indicated airspeeds above 140 miles per hour and highly unstable below this speed. The instability occurred at an angle of attack of about 10° and a normal-force coefficient of about 1.15. When the instability occurred, the airplane tended to pitch up very rapidly even though the elevator was moved down as soon as the pitch up was noticed. The pilots objected to the instability of the airplane in this configuration because of the tendency for the airplane to pitch up to high angles of attack very rapidly. Also, at the high angles of attack violent rolling and yawing motions sometimes occurred.

The data for the flaps-down, landing-gear-down, slats-unlocked configuration are presented in figure 10. The data show that at indicated airspeeds in the range from 140 to 130 miles per hour (angle of attack from 10° to 16°) the airplane has approximately neutral longitudinal stability. At indicated airspeeds slightly less than 130 miles per hour the airplane is very stable longitudinally. In the higher angle-of-attack range (24° to 38°) the data of figure 10(b) indicate that the airplane is again longitudinally unstable. This instability is not very apparent in figure 10(a) because the speed range over which it occurs is very small although the angle-of-attack range for the instability is large. Again, as stated previously, the data at the higher angles of attack only show the trends of the quantities required for trim and balance. As in the case of the flaps-up, slats-unlocked configuration, figure 8, an uncontrolled-for rolling and yawing motion due to stalling was present when the airplane was longitudinally unstable at the high angles of attack (24° to 38°) and again these motions were much more noticeable to the pilots than the longitudinal instability.

Comparison of the longitudinal stability characteristics of the airplane for the four different airplane configurations shows that the slats have a much larger effect on the longitudinal stability than do the flaps. With the slats locked and the flaps up or down the longitudinal stability characteristics of the airplane are very similar and with the slats unlocked and the flaps up or down the characteristics are similar. The slats were very effective in improving the low-speed longitudinal characteristics of the airplane and the pilots had only minor objections to the low-speed longitudinal characteristics when the slats were unlocked.

Higher speeds.- The steady flight longitudinal stability and control characteristics were measured in the Mach number range from about 0.50 to 0.87 with the flaps up, landing gear up, slats locked, and the engine operating at the military power rating of 12,500 rpm. Presented in figure 11 are the variation of elevator position, elevator control force, airplane normal-force coefficient, tail normal-force coefficient, angle of attack, and altitude with Mach number. These data were

obtained in shallow dives which were started at an altitude of about 25,000 feet at a Mach number of about 0.50 and were terminated at an altitude of about 16,000 feet and a Mach number of about 0.87. Data are presented for four different stabilizer settings in the range from 0.7° to 2.8° , stabilizer leading edge up.

For all stabilizer settings a stable variation of elevator position with Mach number occurred, as shown by the decrease in up-elevator deflection or increase in down-elevator deflection required for trim as the Mach number increased. No abrupt trim changes occurred up to the highest Mach number reached, 0.87. In general, for the stabilizer settings used, the elevator control-force variations with Mach number exhibit a stable variation as increasing push forces are required for trim as the Mach number is increased.

From the elevator-position data presented in figure 11 the variation with Mach number of the relative elevator stabilizer effectiveness $\Delta\alpha_T/\Delta\delta_e$ was determined and this variation is presented in figure 12. In the Mach number range from 0.55 to 0.80, $\Delta\alpha_T/\Delta\delta_e$ has a constant value of 0.4. Between Mach numbers of 0.80 and 0.85 the data indicate a slight decrease in $\Delta\alpha_T/\Delta\delta_e$.

Longitudinal Characteristics in Accelerated Flight

The longitudinal stability and control characteristics of the Douglas D-558-II airplane in accelerated flight were measured in wind-up turns in the Mach number range from 0.40 to 0.87. Turns were made with the slats both locked and unlocked.

Time histories of two turns made at a Mach number of approximately 0.60 with the slats locked are presented in figures 13 and 14. Inspection of figure 13 shows that for airplane normal-force coefficients less than 0.7 to 0.8 (before time 11.0 sec) the airplane is stable since increasing up-elevator deflections are required to increase the airplane normal-force coefficient. At times between about 11 and 12.8 seconds the data indicate that the airplane is unstable. Although the elevator was held substantially fixed, the airplane pitched up quite violently. The angle of attack increased from 6° to 23° and the pitching velocity from 0.25 radian per second to 0.6 radian per second. At the same time the normal acceleration increased from 4.0g to 5.0g and the normal-force coefficient from 0.70 to 0.95. The pilot applied corrective elevator control soon after the pitch up occurred and overcontrolled the airplane in recovering. A negative normal acceleration of about 3.0g was reached during the recovery. No unusual lateral or directional airplane motions occurred during this turn and therefore these motions are not presented in the time history.

In the turn shown by the time history of figure 14 the pilot attempted to fly the airplane in the normal-force-coefficient range where the airplane was unstable (times between 11 and 14 sec). After the airplane pitched up, the airplane first performed an unsteady rolling motion. The pilot used the rudder in attempting to control this rolling motion and caused the airplane to perform a 360° snaproll. The data indicate that very large angles of sideslip were reached during the snaproll. No sideslip-angle measurements were obtained during the maneuver, but integration of the yawing velocity indicates that sideslip angles on the order of 30° to 35° were approached. A maximum lateral acceleration of about 1.1g occurred during the snaproll. This lateral acceleration corresponds to a side force on the airplane of about 10,800 pounds. The distribution of the side force on the airplane between the fuselage and vertical tail is not known, but it is likely that the load on the vertical tail, during oscillatory yawed flight, approached the vertical tail design limit load of 8,700 pounds. The maximum rolling velocity which occurred during the snaproll is not known as the 2.6-radian-per-second range of the rolling-velocity recorder was exceeded, but it is likely that the maximum rolling velocity was on the order of 3.5 to 4.0 radians per second. In recovering from the snaproll the airplane again reached a negative normal acceleration of 3.0g.

The pilots reported and the recording instruments showed that airplane buffeting occurred at normal accelerations slightly less than the acceleration at which the airplane became unstable. This buffeting served as a warning of the approach of instability. If the elevator is moved down when the airplane buffeting occurs, the response of the airplane is good and the instability can be avoided. In the pilot's opinion the airplane is unflyable in accelerated flight in the lift-coefficient range in which it is unstable. If the pitch up resulting from the instability is not checked by moving the elevator down as soon as it is noticed by the pilot, the angle of attack increases very rapidly and violent rolling and yawing motions occur when the high angles of attack are reached.

The longitudinal instability occurred in turns with the slats locked in the Mach number range from 0.40 to 0.65. In this Mach number range there was little if any change in the normal-force coefficient of 0.7 to 0.8 at which the instability occurred. No information has as yet been obtained on the longitudinal stability and control characteristics of the Douglas D-558-II airplane at high lift coefficients at Mach numbers greater than about 0.65. Because of the power limitation of the airplane with only the jet engine installed, it was not possible to make turns at high Mach numbers and high altitudes so as to obtain high airplane lift coefficients with reasonable load factors. It may be pointed out that, with the same wing loading, the normal-force coefficient at which instability occurs corresponds to a maneuvering load factor of less than 1g at an altitude of 40,000 feet and a Mach number of 0.65.

Presented in figure 15 is a time history of a turn made at a Mach number of about 0.60 with the airplane in the slats-unlocked configuration. The data of figure 15 indicate that with the slats unlocked the airplane is stable to higher normal-force coefficients than with the slats locked, the normal-force coefficient for instability being about 0.90. Also, the pitch up which occurs when the airplane becomes unstable is mild when compared with the slats-locked configuration. In no case, in turns with the slats unlocked, have violent uncontrollable yawing and rolling motions occurred after the pitch up as did occur with the slats locked. The pilots did not consider the degree of instability present with the slats unlocked to be nearly as objectionable as the instability with the slats locked.

From turns such as were presented as time histories in figures 13, 14, and 15 the variations of elevator position, tail normal-force coefficient, and airplane normal-force coefficient with angle of attack, the variations of elevator position and tail normal-force coefficient with airplane normal-force coefficient, and the variation of elevator control force with normal acceleration were determined. These data are presented in figure 16 for Mach numbers of approximately 0.40, 0.62, 0.74, and 0.87 with the airplane in the slats-locked configuration. Similar data for the slats-unlocked configuration are presented in figure 17 for Mach numbers of approximately 0.40, 0.60, and 0.85. The variation of the slat position with angle of attack is also presented in figure 17.

At the lower lift coefficients where the airplane was longitudinally stable, the variations of the elevator position with airplane normal-force coefficient or angle of attack and elevator control force with normal acceleration are substantially linear. In the normal-force-coefficient range where the airplane was unstable the pilots were not able to trim or balance the airplane in accelerated flight. Therefore, the data presented in figures 16 and 17 for this normal-force-coefficient range represent only the quantities for the particular maneuver and may or may not be quantities required to trim or balance the airplane.

At the lower angles of attack there is no measurable difference in the longitudinal stability or control between the slats-locked and the slats-unlocked configurations. It is of interest to note that, in the turn made in the Mach number range from 0.85 to 0.77, figure 17(c), the slats although unlocked did not open as the angle of attack was increased during the turn. At an angle of attack of 3.7 and a Mach number of 0.77, figure 17(c), the slat opening was about 0.1 inch; whereas at the same angle of attack at a Mach number of 0.60, figure 17(b), the slat opening was about 2 inches.

Presented in figure 18 are the variations with Mach numbers of $d\delta_e/dC_{N_A}$, the elevator deflection required to produce a unit change in

normal-force coefficient, and $\Delta F_e/\Delta g$, the elevator control force per g of acceleration. The values of $d\delta_e/dC_{N_A}$ and $\Delta F_e/\Delta g$ presented are for the low-lift-coefficient range where the airplane was longitudinally stable and are for turning flight. In the Mach number range from 0.4 to 0.6 the values of $d\delta_e/dC_{N_A}$ and $\Delta F_e/\Delta g$ are substantially constant at 10.0. In the Mach number range from 0.6 to 0.87, the values of $d\delta_e/dC_{N_A}$ and $\Delta F_e/\Delta g$ increase and at a Mach number of 0.87 $d\delta_e/dC_{N_A}$ and $\Delta F_e/\Delta g$ have a value of about 19.0. As was pointed out previously in the paper from the data of figure 12, the elevator effectiveness at a Mach number of 0.85 is only slightly less than at a Mach number of 0.60 and, therefore, most of the increase in $d\delta_e/dC_{N_A}$ and $\Delta F_e/\Delta g$ which occurs as the Mach number is increased from 0.60 to 0.85 can be attributed to an increase in stability of the airplane. From measurements of the horizontal-tail loads it is shown that the increase in the airplane stability can be attributed to the increase in the stability of the wing-fuselage combination. A measure of the stability of the wing-fuselage combination is presented in figure 19 as the variation of the aerodynamic center of the wing-fuselage combination with Mach number. These data are for low normal-force coefficients and were obtained from the tail-load slopes, as shown in typical plots of figures 16 and 17. The tail loads have been corrected for the effect of pitching acceleration. Inspection of figure 19 shows that the aerodynamic center of the wing-fuselage combination moves rearward as the Mach number increases. At a Mach number of 0.40 the aerodynamic center is at about 10 percent of the mean aerodynamic chord and at a Mach number of 0.87 the aerodynamic center is at about 20 percent of the mean aerodynamic chord.

CONCLUDING REMARKS

Flight measurements were made with the Douglas D-558-II research airplane to determine the longitudinal stability and control characteristics in both steady flight and accelerated flight.

With the slats locked and the flaps up, the airplane was longitudinally unstable at normal-force coefficients greater than approximately 0.8 in steady flight at low speeds and in maneuvering flight at Mach numbers up to at least 0.65. No data were obtained at high normal-force coefficients at Mach numbers greater than about 0.65 because of the power limitations of the airplane with only the jet engine installed. The instability proved objectionable to the pilots, particularly in accelerated flight because of the tendency for the airplane to pitch to high angles of attack very rapidly and because violent rolling and yawing motions sometimes occurred when the high angles of attack were reached. The instability probably resulted from a large increase in the

rate of change of effective downwash at the tail with increase in angle of attack at moderate and high angles of attack.

With the flaps down and the slats locked the longitudinal stability characteristics in steady flight at low speeds were very similar to the characteristics with the flaps up and the slats locked except that the instability occurred at a higher normal-force coefficient.

The degree of instability present with the slats unlocked and the flaps up or down was much less than with the slats locked and the pilots had only minor objections to the longitudinal characteristics of the airplane.

In steady flight in the Mach number range from 0.50 to 0.87 the airplane was stable longitudinally and no abrupt trim changes occurred up to the highest Mach number reached, 0.87. The data indicate that only a slight reduction in the relative elevator-stabilizer effectiveness occurred in going from a Mach number of about 0.55 to 0.85.

In turning flight at low lift coefficients the values of $d\delta_e/dC_{N_A}$ and $\Delta F_e/\Delta g$ were approximately doubled as the Mach number was increased from 0.6 to 0.87. Most of the increase in $d\delta_e/dC_{N_A}$ and $\Delta F_e/\Delta g$ can be attributed to an increase in the stability of the airplane which occurred because of the increase in the stability of the wing-fuselage combination. At a Mach number of 0.4 the aerodynamic center of the wing-fuselage combination is at about 10 percent of the mean aerodynamic chord and at a Mach number of 0.87 the aerodynamic center is at about 20 percent of the mean aerodynamic chord.

Langley Aeronautical Laboratory
National Advisory Committee for Aeronautics
Langley Field, Va.

REFERENCES

1. Sjoberg, S. A.: Flight Measurements with the Douglas D-558-II (BuAero No. 37974) Research Airplane. Static Lateral and Directional Stability Characteristics as Measured in Sideslips at Mach Numbers up to 0.87. NACA RM L50C14, 1950.
2. Mayer, John P., Valentine, George M., and Mayer, Geraldine C.: Flight Measurements with the Douglas D-558-II (BuAero No. 37974) Research Airplane. Determination of the Aerodynamic Center and Zero-Lift Pitching-Moment Coefficient of the Wing-Fuselage Combination by Means of Tail-Load Measurements in the Mach Number Range from 0.37 to 0.87. NACA RM L50D10, 1950.
3. Mayer, John P., and Valentine, George M.: Flight Measurements with the Douglas D-558-II (BuAero No. 37974) Research Airplane. Measurements of the Buffet Boundary and Peak Airplane Normal-Force Coefficients at Mach Numbers up to 0.90. NACA RM L50E31, 1950.
4. Wilmerding, J. V., Stillwell, W. H., and Sjoberg, S. A.: Flight Measurements with the Douglas D-558-II (BuAero No. 37974) Research Airplane. Lateral Control Characteristics as Measured in Abrupt Aileron Rolls at Mach Numbers up to 0.86. NACA RM L50E17, 1950.
5. Stillwell, W. H., Wilmerding, J. V., and Champine, R. A.: Flight Measurements with the Douglas D-558-II (BuAero No. 37974) Research Airplane. Low-Speed Stalling and Lift Characteristics. NACA RM L50G10, 1950.
6. Mayer, John P., and Valentine, George M.: Flight Measurements with the Douglas D-558-II (BuAero No. 37974) Research Airplane. Measurements of the Distribution of the Aerodynamic Load among the Wing, Fuselage, and Horizontal Tail at Mach Numbers up to 0.87. NACA RM L50J13, 1950.
7. Mayer, John P., Valentine, George M., and Swanson, Beverly J.: Flight Measurements with the Douglas D-558-II (BuAero No. 37974) Research Airplane. Measurements of Wing Loads at Mach Numbers up to 0.87. NACA RM L50H16, 1950.
8. Thompson, F. L., and Zalovcik, John A.: Airspeed Measurements in Flight at High Speeds. NACA ARR, Oct. 1942.
9. Danforth, Edward C. B., and Johnston, J. Ford: Error in Airspeed Measurements Due to Static-Pressure Field ahead of Sharp-Nose Bodies of Revolution at Transonic Speeds. NACA RM L9C25, 1949.

10. Kerker, R., and Miller, C. E.: Summary Report of Model D-558-2 Tests at Cooperative Wind Tunnel. Rep. No. ES-20648, Douglas Aircraft Co., Inc., Oct. 1, 1946.
11. Furlong, G. Chester, and Bollech, Thomas V.: Downwash, Sidewash, and Wake Surveys behind a 42° Sweptback Wing at a Reynolds Number of 6.8×10^6 with and without a Simulated Ground. NACA RM L8G22, 1948.

TABLE I
 DIMENSIONS AND CHARACTERISTICS OF THE
 DOUGLAS D-558-II AIRPLANE

Wing:

Root airfoil section (normal to 0.30 chord)	NACA 63-010
Tip airfoil section (normal to 0.30 chord)	NACA 63 ₁ -012
Total area, sq ft	175.0
Span, ft	25.0
Mean aerodynamic chord, in.	87.3
Root chord (parallel to plane of symmetry), in.	108.5
Tip chord (parallel to plane of symmetry), in.	61.2
Taper ratio	0.565
Aspect ratio	3.570
Sweep at 0.30 chord, deg	35.0
Incidence at fuselage center line, deg	3.0
Dihedral, deg	-3.0
Geometric twist, deg	0
Total aileron area (rearward of hinge), sq ft	9.8
Aileron span, perpendicular to plane of symmetry, in.	66
Aileron travel (each), deg	±15
Total flap area, sq ft	12.58
Flap travel, deg	50

Horizontal tail:

Root airfoil section (normal to 0.30 chord)	NACA 63-010
Tip airfoil section (normal to 0.30 chord)	NACA 63-010
Area (including fuselage), sq ft	39.9
Span, in.	143.6
Mean aerodynamic chord, in.	41.75
Root chord (parallel to plane of symmetry), in.	53.6
Tip chord (parallel to plane of symmetry), in.	26.8
Taper ratio	0.50
Aspect ratio	3.59
Sweep at 0.30 chord line, deg	40.0
Dihedral, deg	0
Elevator area, sq ft	9.4
Elevator travel, deg	25 up, 15 down
Stabilizer travel, deg	4 L.E. up, 5 L.E. down



TABLE I
 DIMENSIONS AND CHARACTERISTICS OF THE
 DOUGLAS D-558-II AIRPLANE - Concluded

Vertical tail:	
Airfoil section (parallel to fuselage center line)	NACA 63-010
Area, sq ft	36.6
Height from fuselage center line, in.	98.0
Root chord (parallel to fuselage center line), in.	146.0
Tip chord (parallel to fuselage center line), in.	44.0
Sweep angle at 0.30 chord, deg	49.0
Rudder area (rearward of hinge line), sq ft	6.15
Rudder travel, deg	±25
Fuselage:	
Length, ft	42.0
Maximum diameter, in.	60.0
Fineness ratio	8.40
Speed-retarder area, sq ft	5.25
Power plant	J-34-WE-40
	2 jatos for take-off
Airplane weight (full fuel), lb	10,645
Airplane weight (no fuel), lb	9,085
Airplane weight (full fuel and 2 jatos), lb	11,060
Center-of-gravity locations:	
Full fuel (gear down), percent mean aerodynamic chord	25.3
Full fuel (gear up), percent mean aerodynamic chord	25.8
No fuel (gear down), percent mean aerodynamic chord	26.8
No fuel (gear up), percent mean aerodynamic chord	27.5
Full fuel and 2 jatos (gear down), percent mean aerodynamic chord	29.2



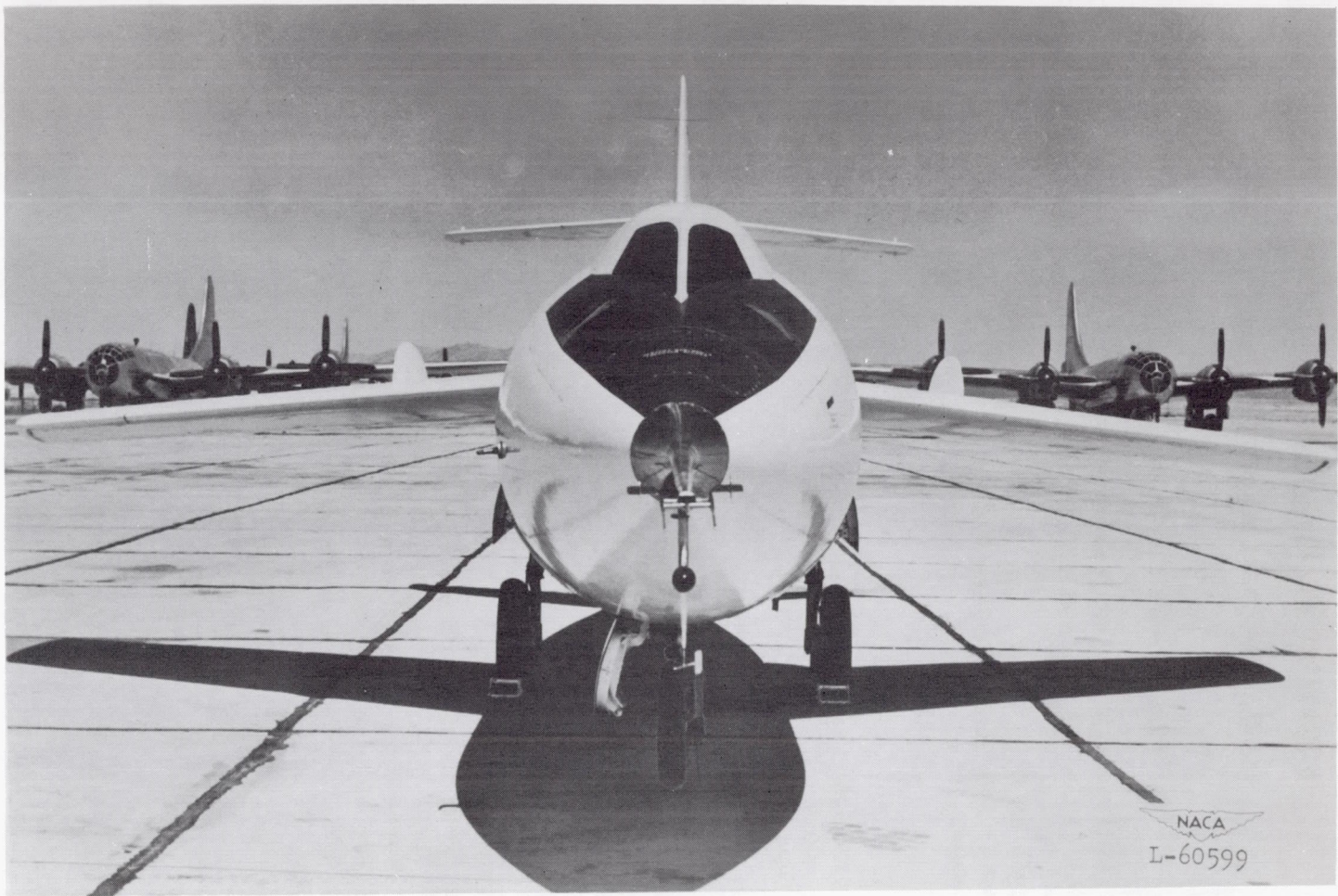
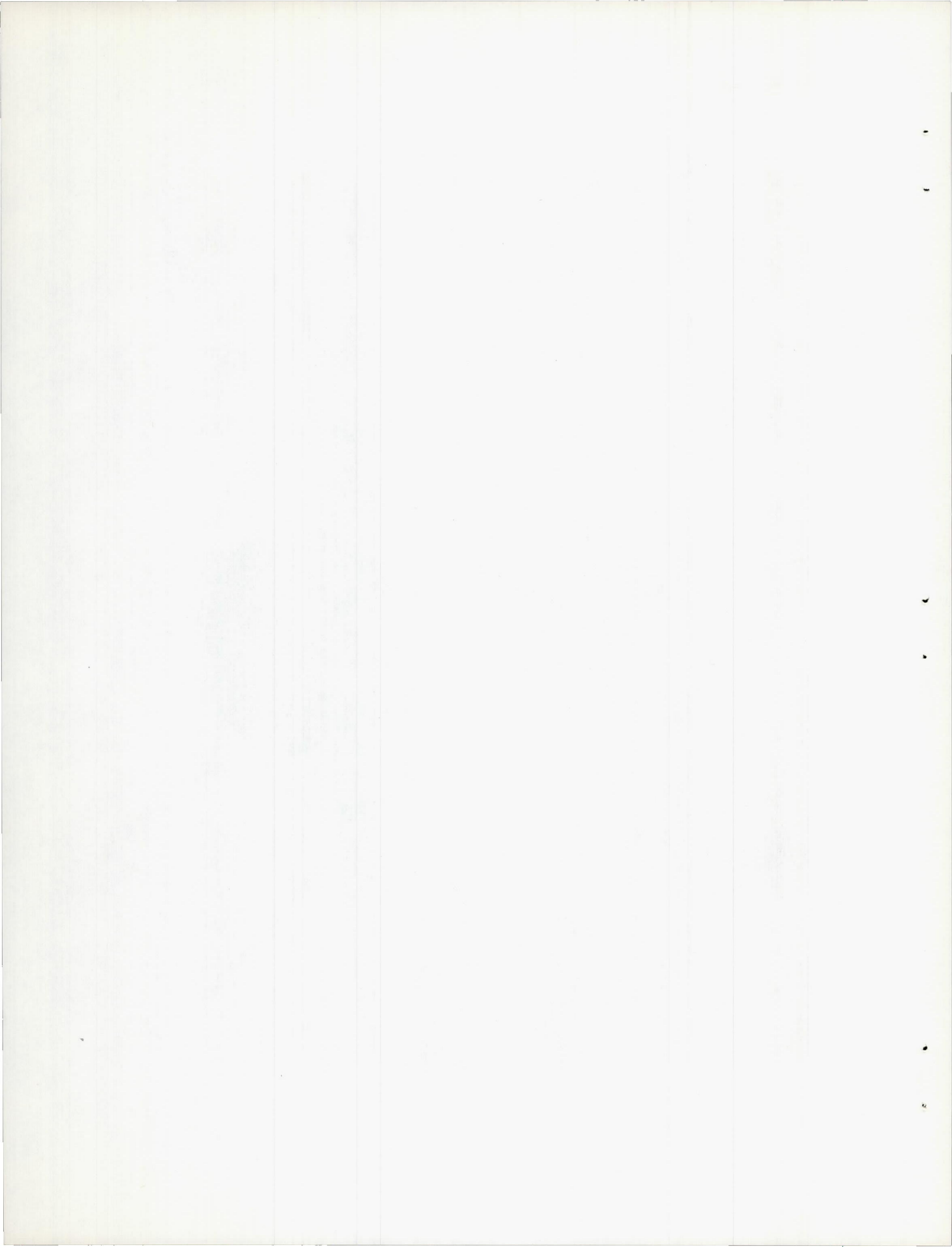


Figure 1.- Front view of Douglas D-558-II (BuAero No. 37974) research airplane.



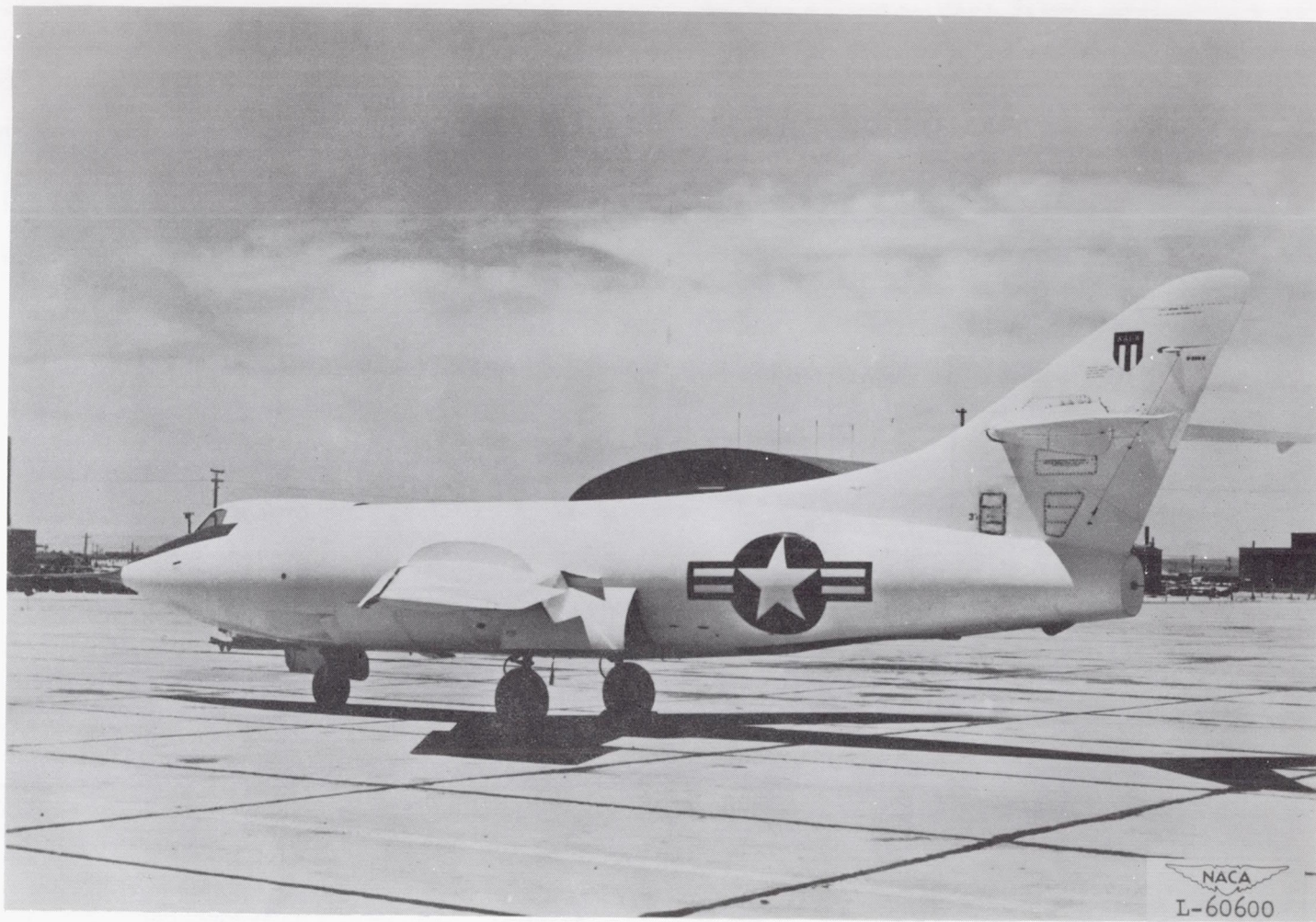
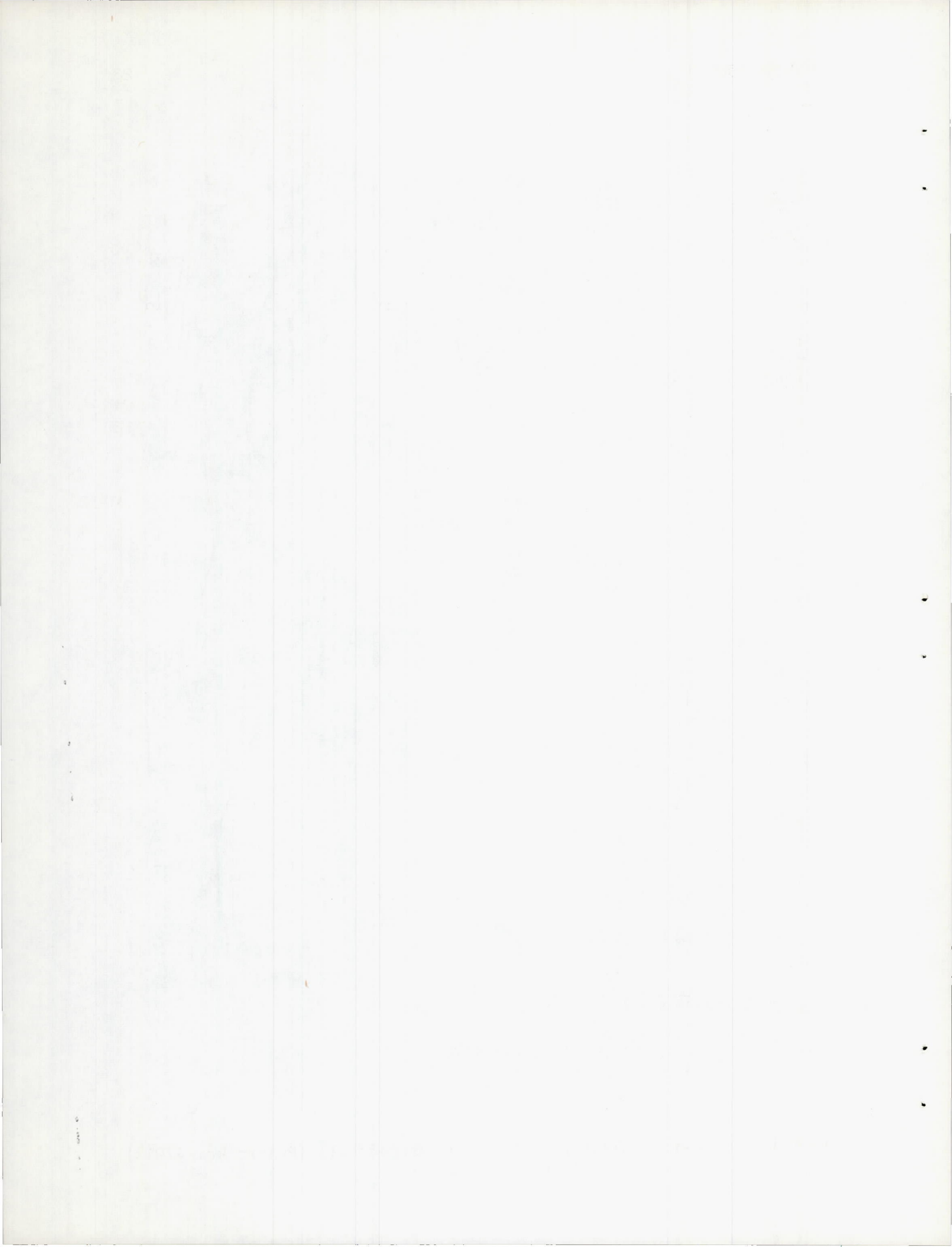


Figure 2.- Three-quarter rear view of Douglas D-558-II (BuAero No. 37974) research airplane.



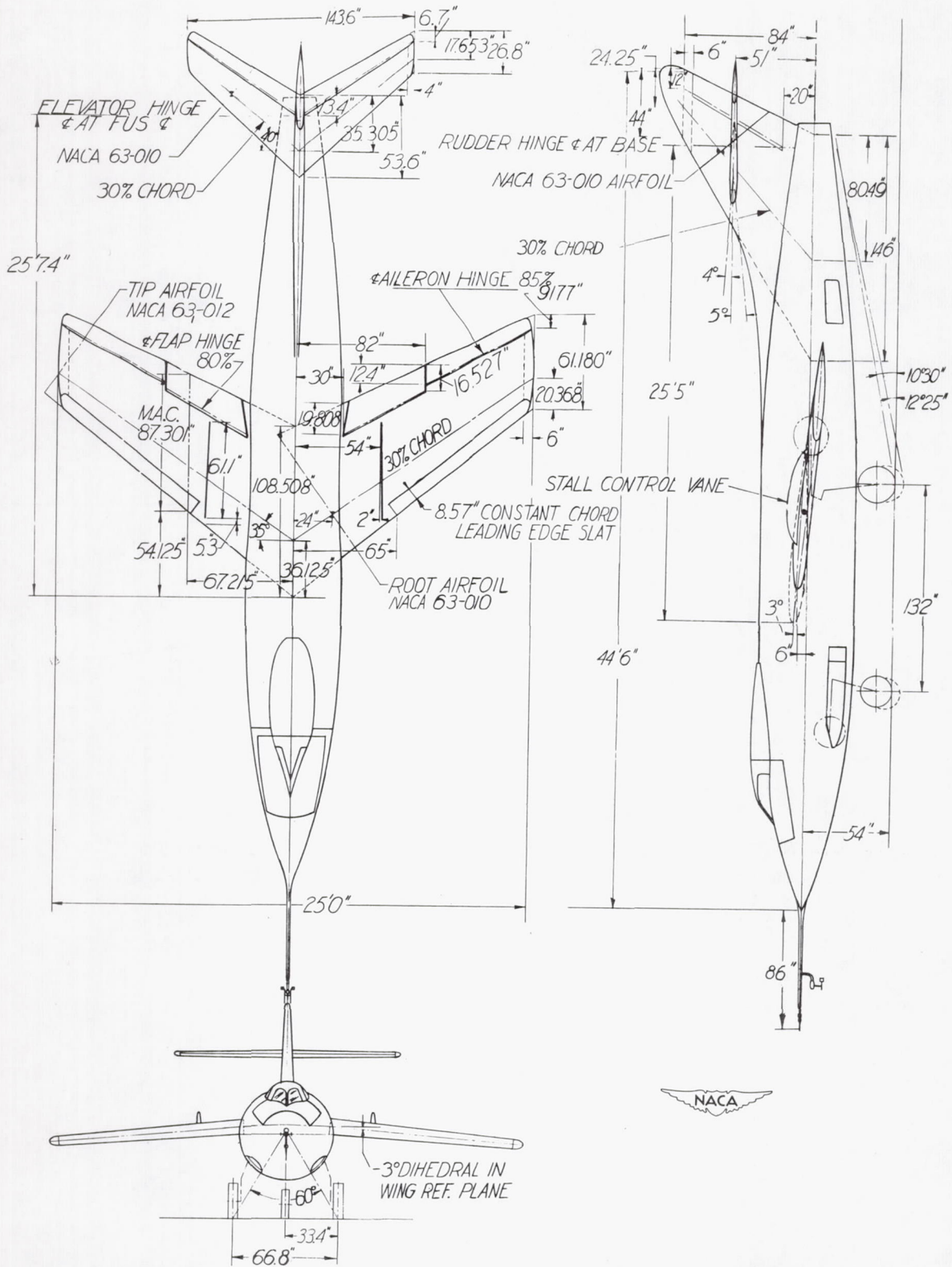


Figure 3.- Three-view drawing of the Douglas D-558-II (BuAero No. 37974) research airplane.

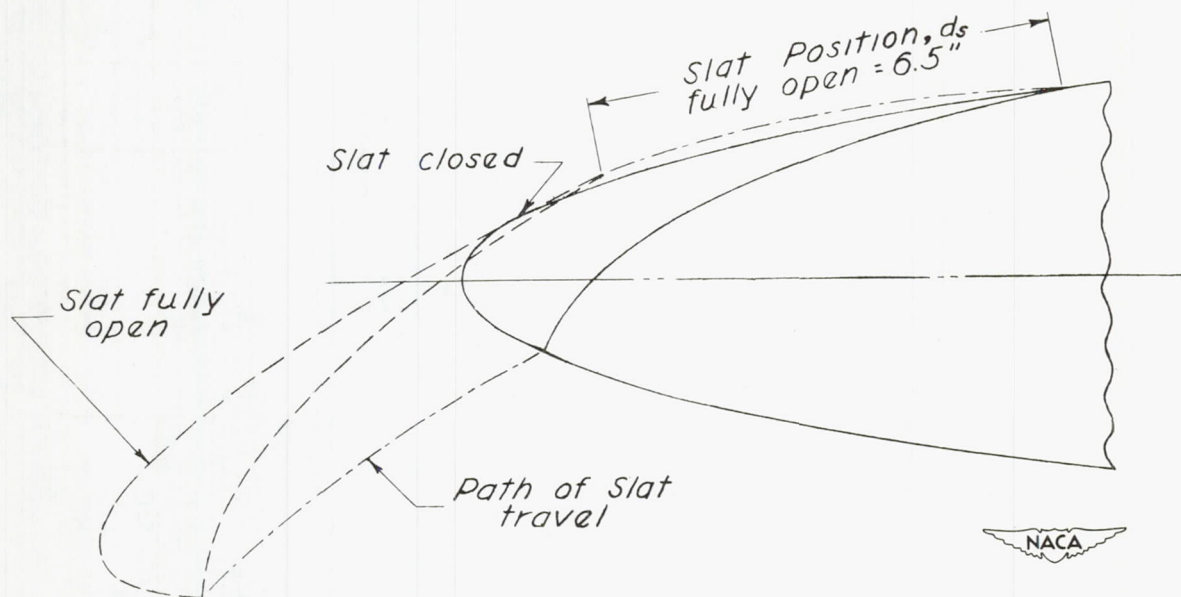


Figure 4.- Section of wing slat of Douglas D-558-II (BuAero No. 37974) research airplane perpendicular to leading edge of wing.

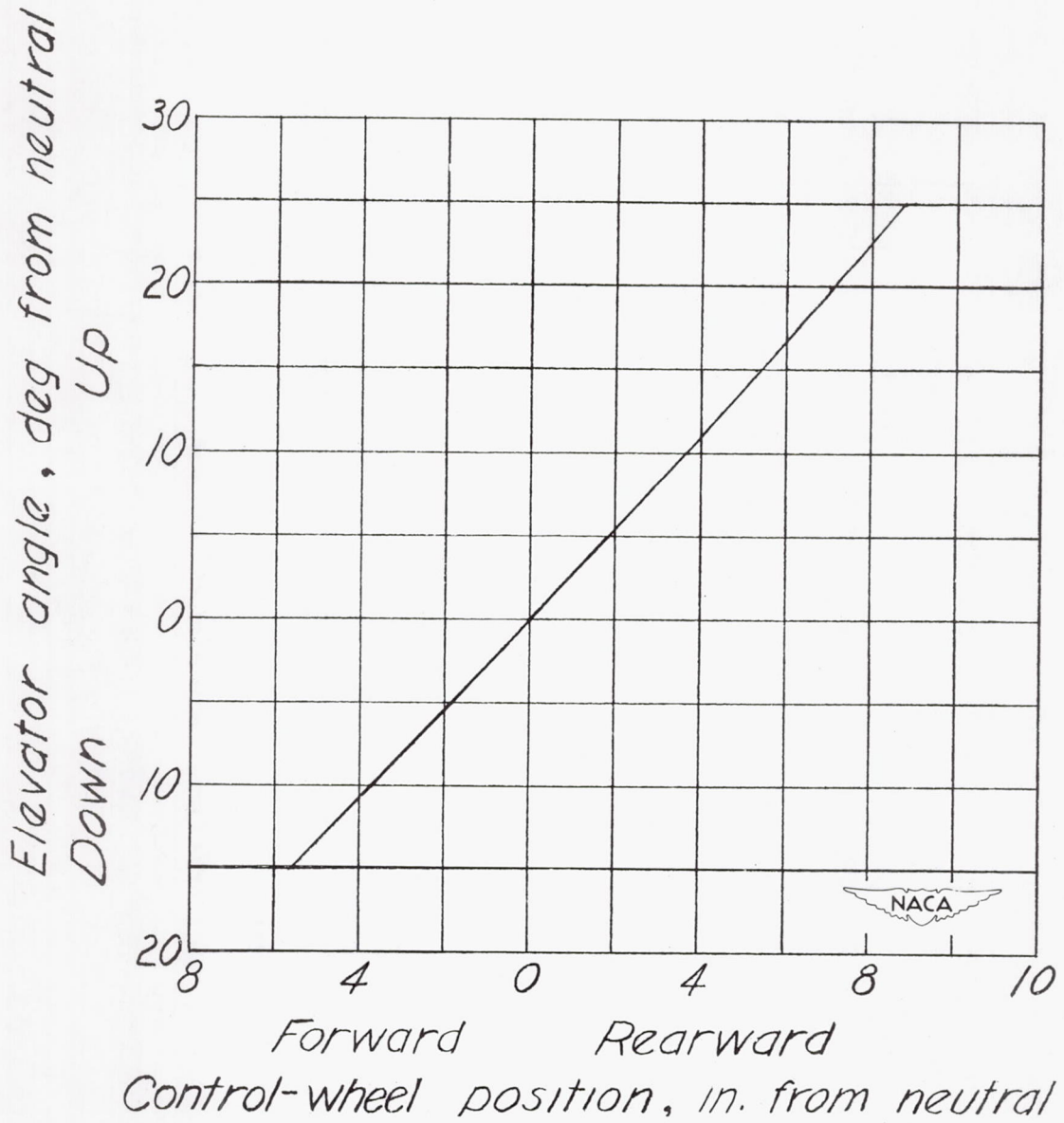


Figure 5.- Variation of elevator position with control-wheel position.
No load on system.

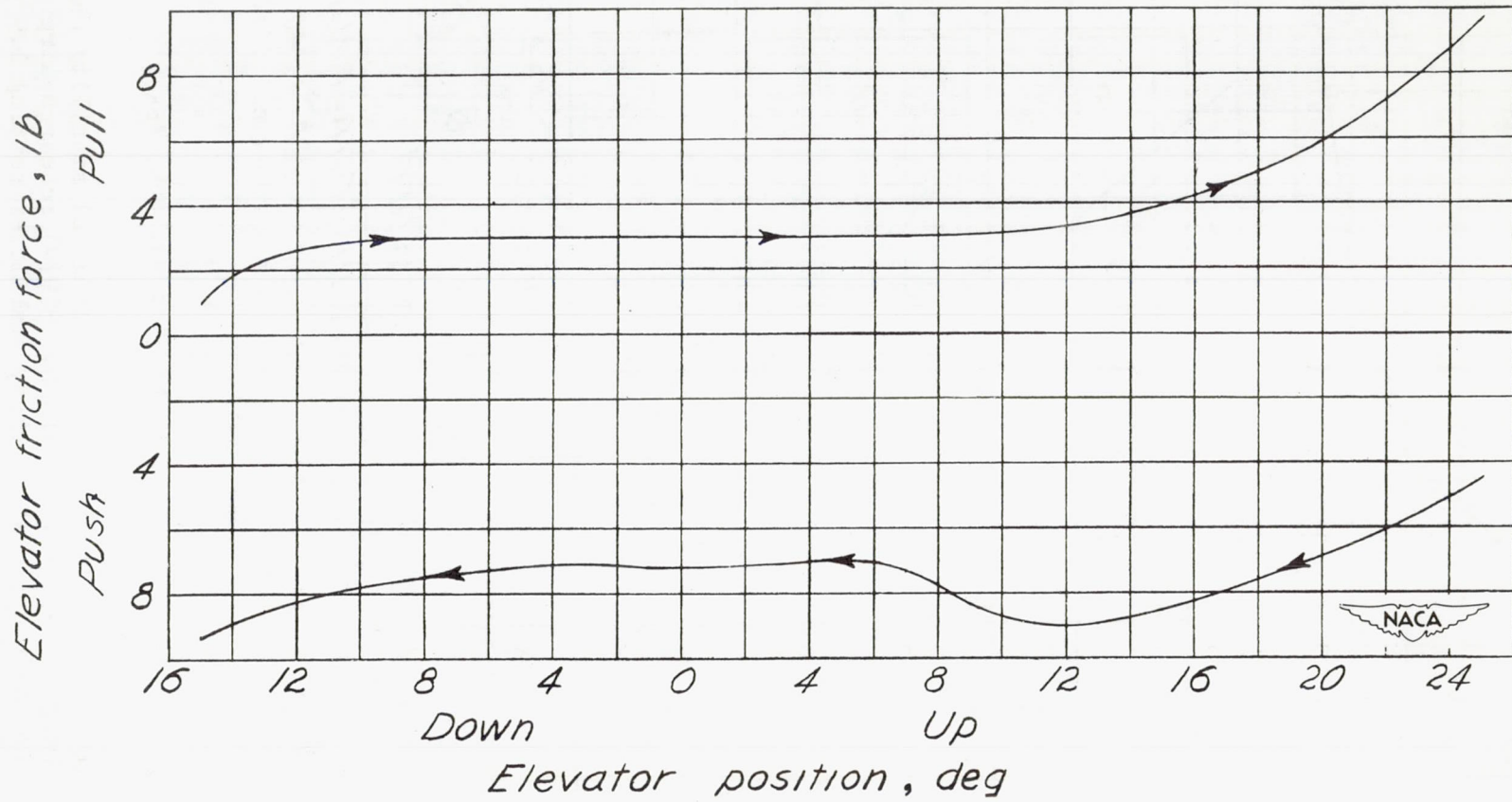
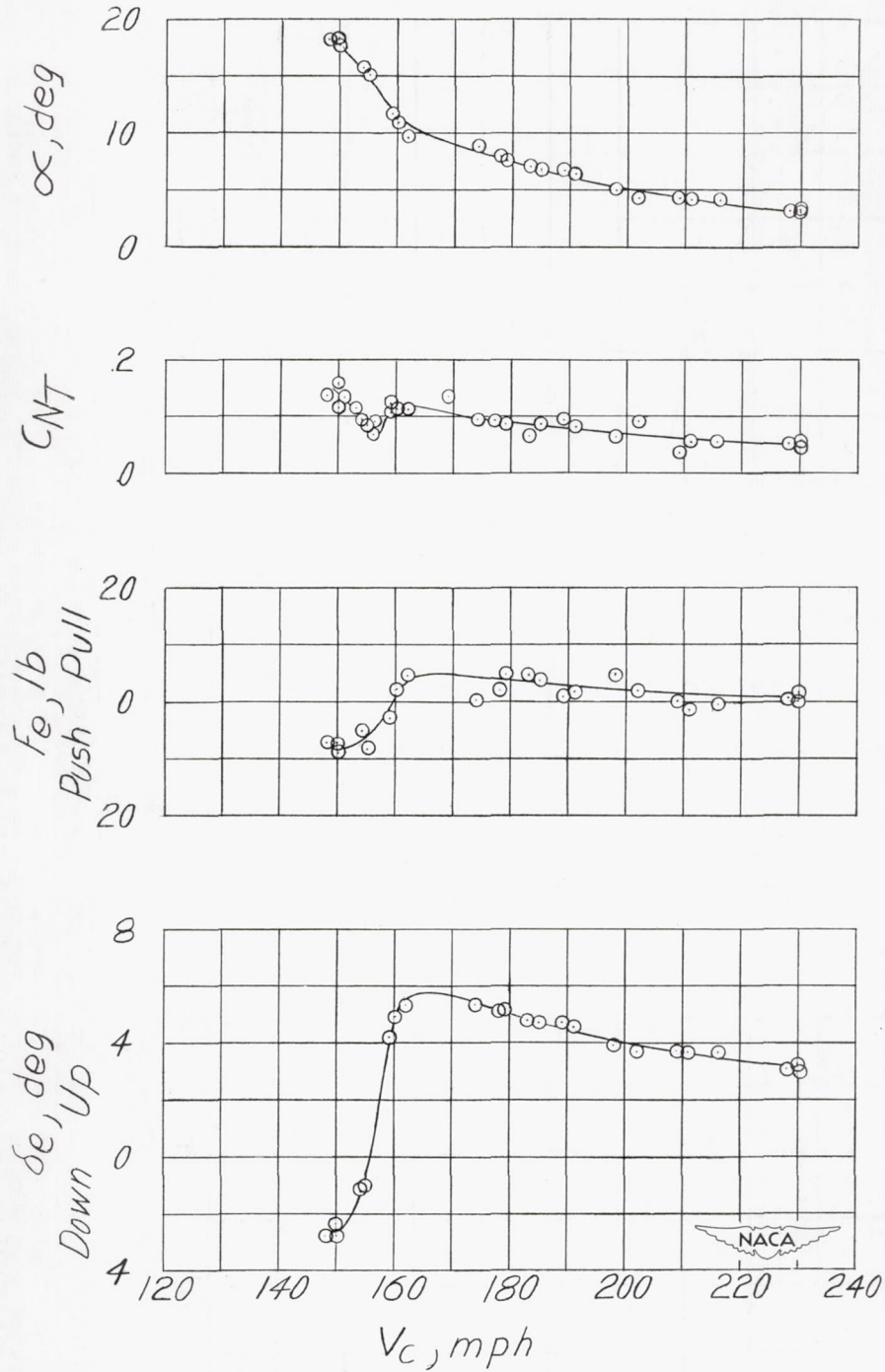
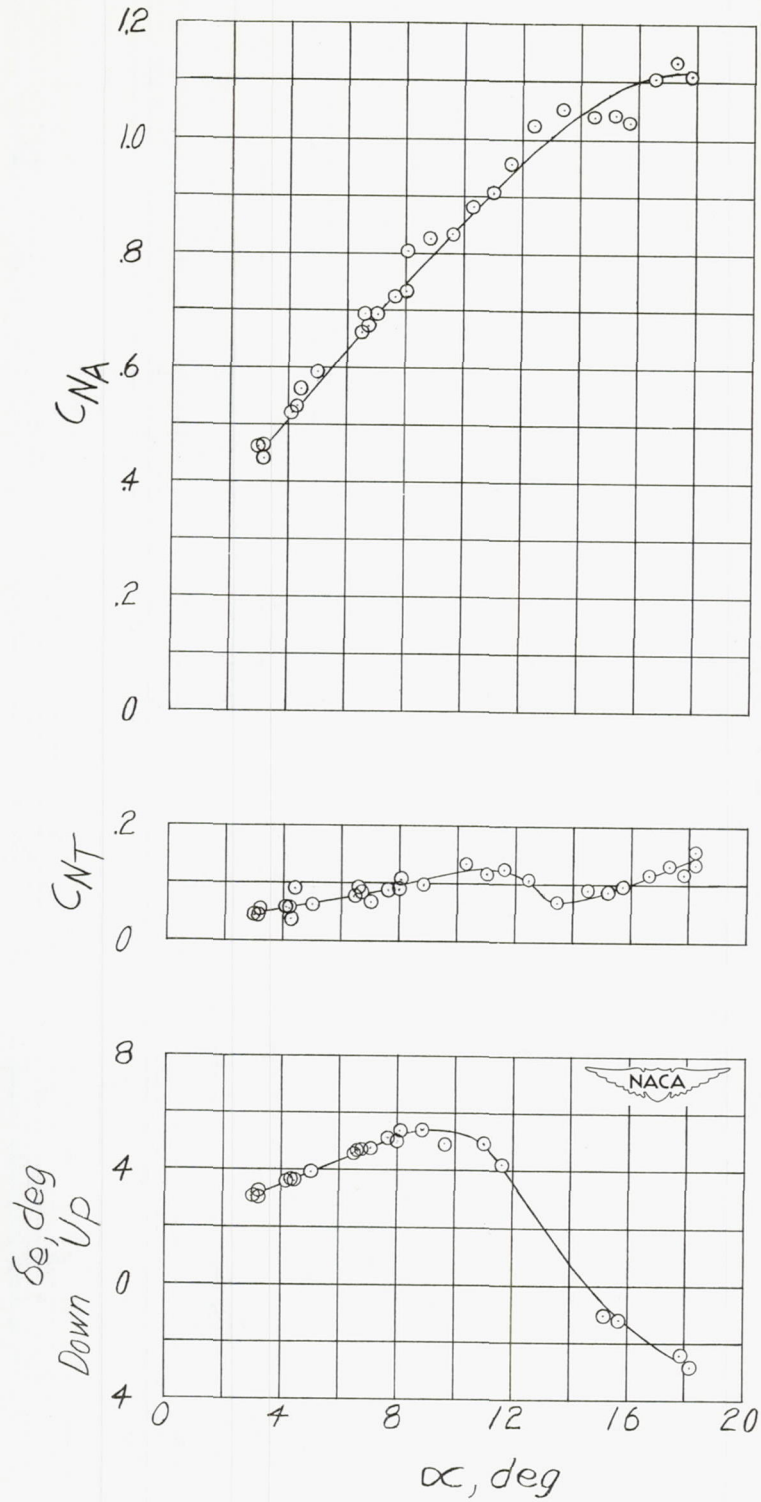


Figure 6.- Elevator control force required to deflect elevator on the ground under no load.



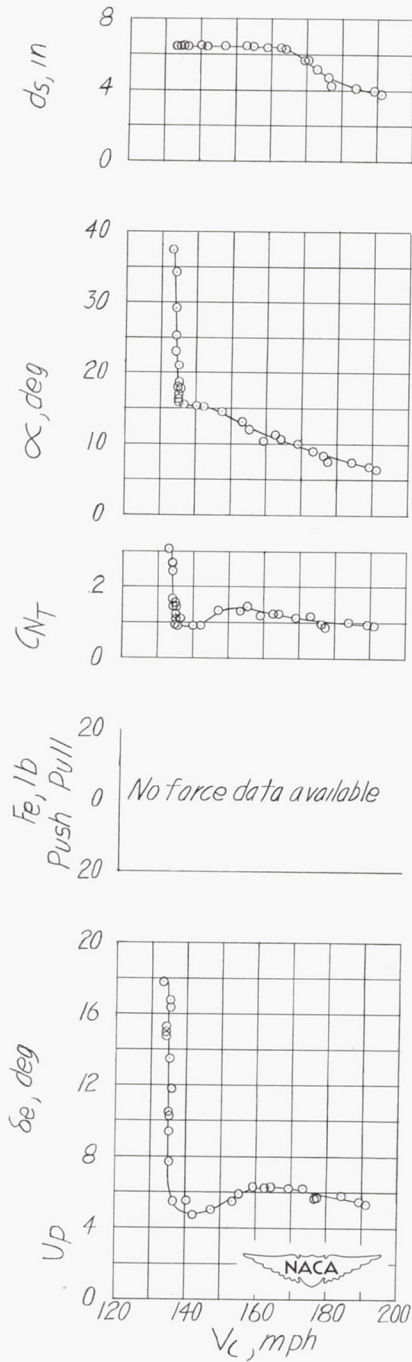
(a) δ_e , F_e , C_{N_T} , and α plotted against V_c .

Figure 7.- Low-speed steady flight static longitudinal stability characteristics of the Douglas D-558-II (BuAero No. 37974) research airplane. Flaps up; landing gear up; slats locked; stabilizer setting 1.9° ; center of gravity at 26.6 percent mean aerodynamic chord.



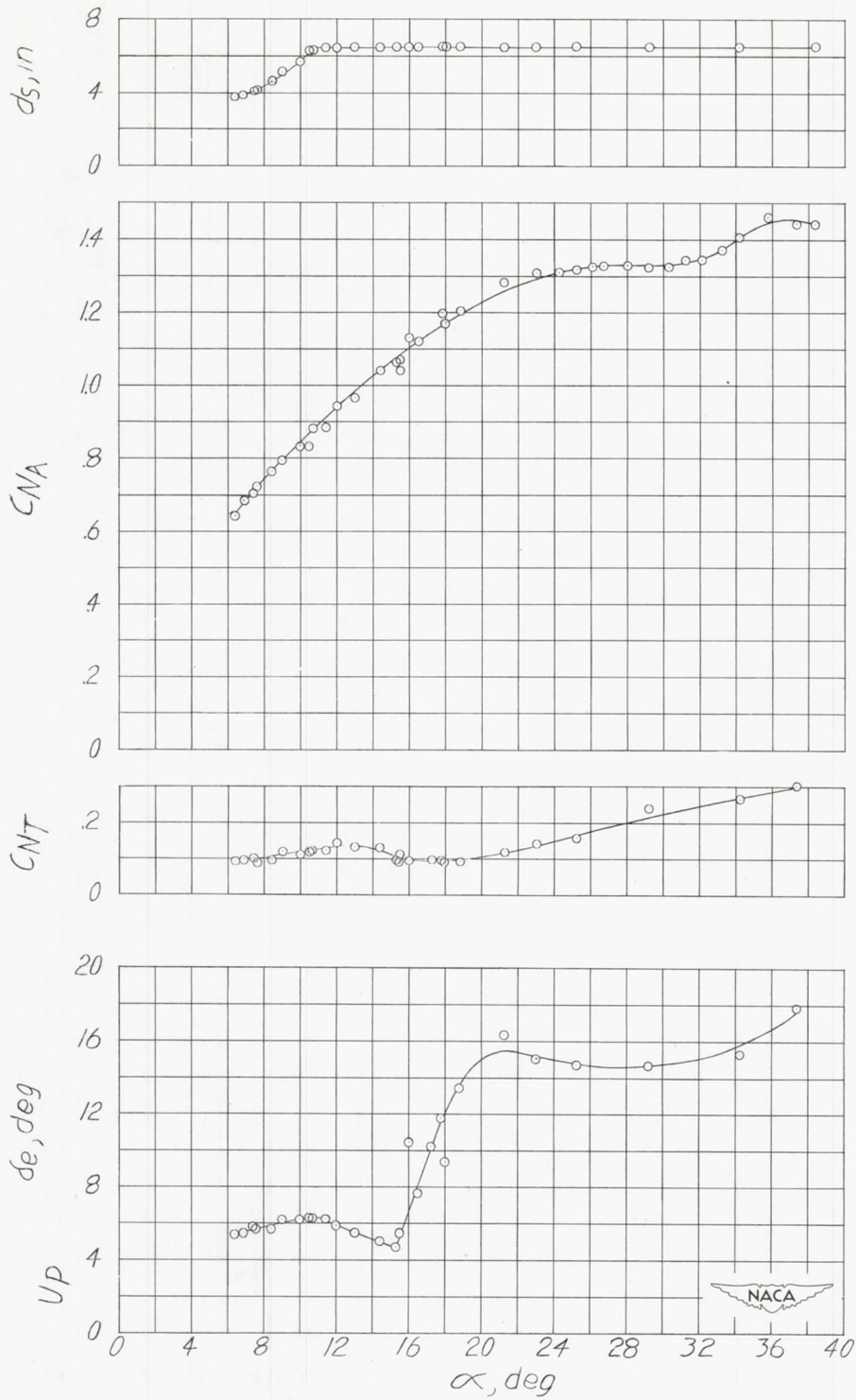
(b) δ_e , C_{NT} , and C_{NA} plotted against α .

Figure 7.- Concluded.



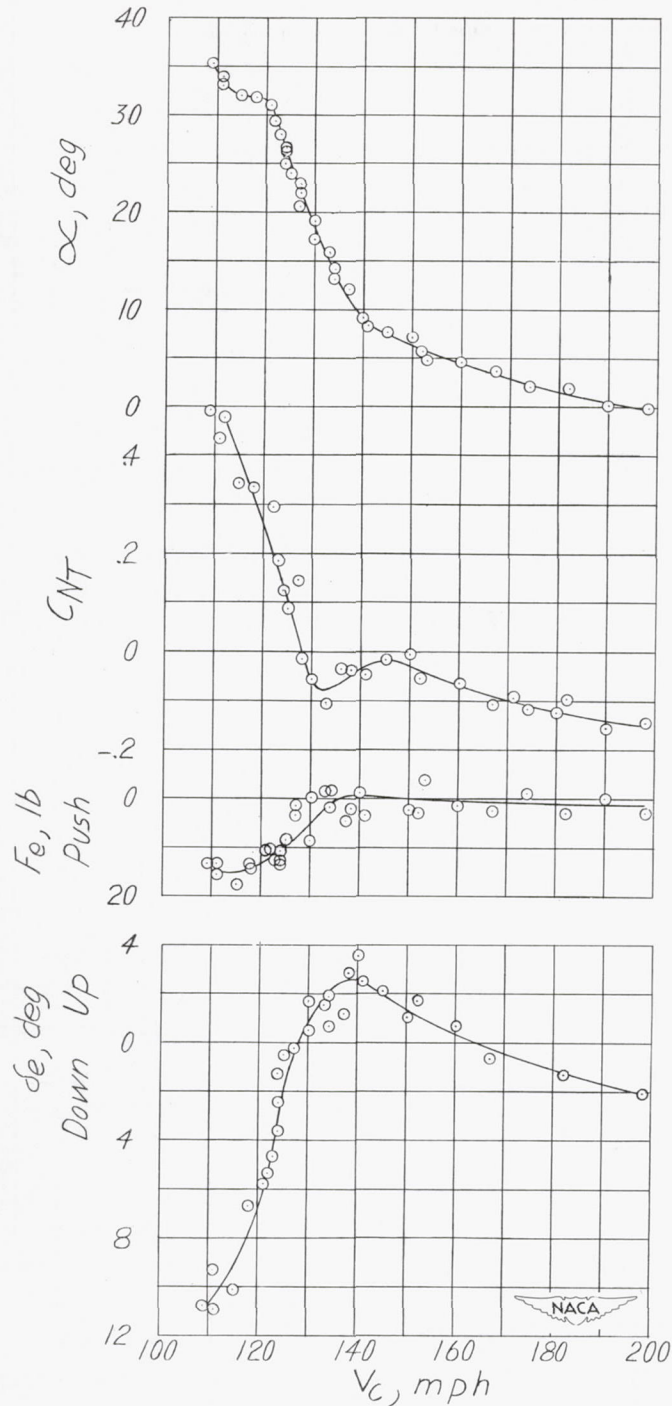
(a) δ_e , F_e , C_{N_T} , α , and d_s plotted against V_c .

Figure 8.- Low-speed steady flight static longitudinal stability characteristics of the Douglas D-558-II (BuAero No. 37974) research airplane. Flaps up; landing gear up; slats unlocked; stabilizer setting 1.7° ; center of gravity at 26.7 percent mean aerodynamic chord.



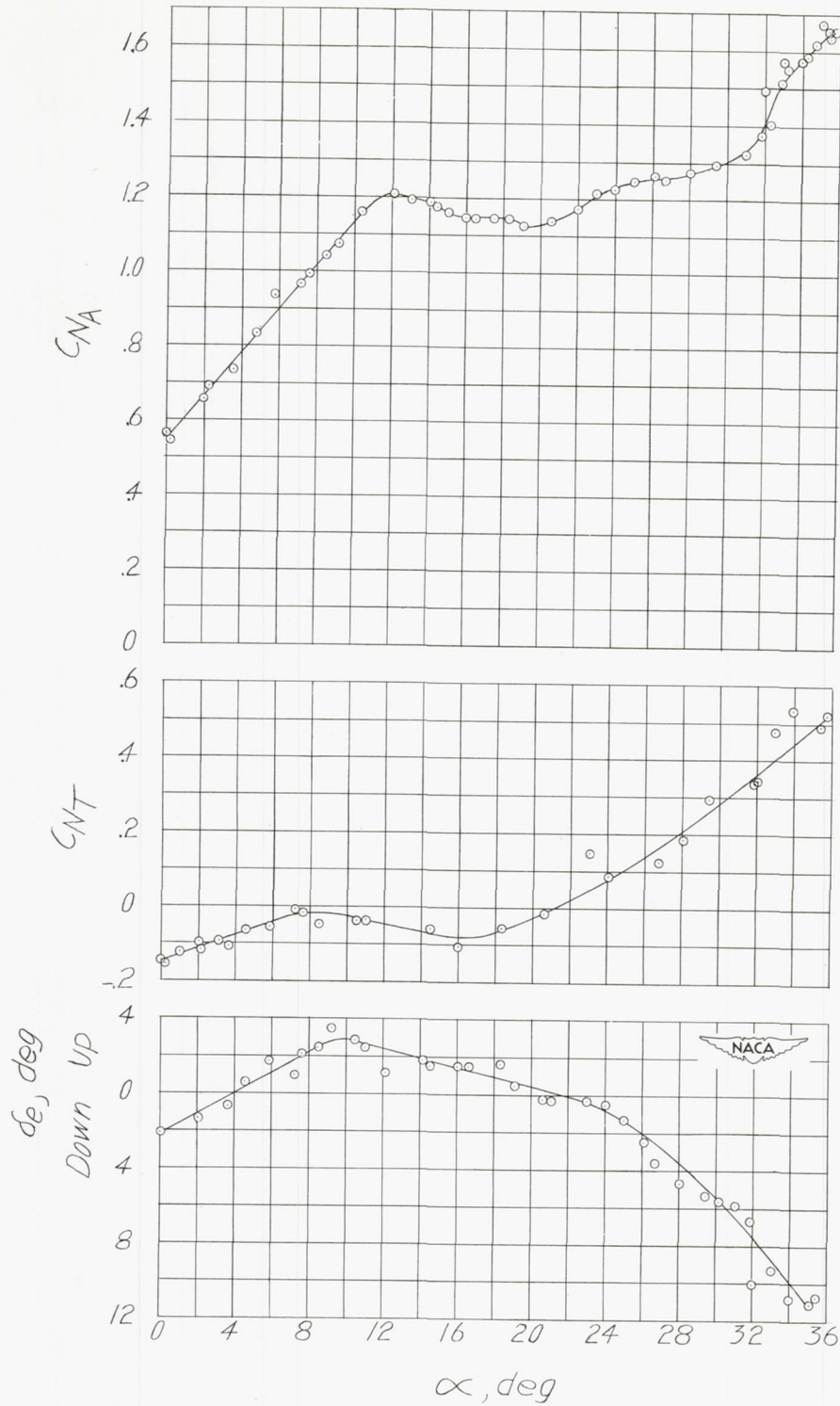
(b) δ_e , C_{NT} , C_{NA} , and d_s plotted against α .

Figure 8.- Concluded.



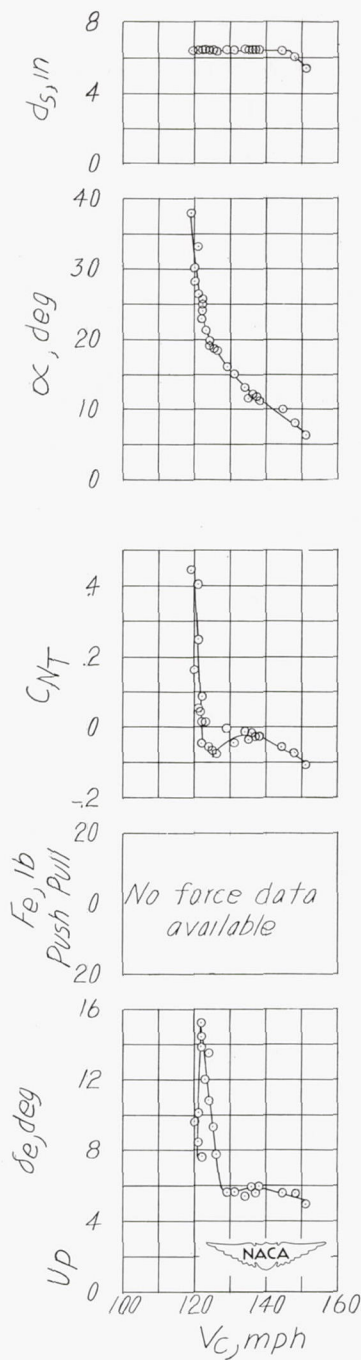
(a) δ_e , F_e , C_{N_T} , and α plotted against V_c .

Figure 9.- Low-speed steady flight static longitudinal stability characteristics of the Douglas D-558-II (BuAero No. 37974) research airplane. Flaps down; landing gear down; slats locked; stabilizer setting 0.7° ; center of gravity at 27.1 percent mean aerodynamic chord.



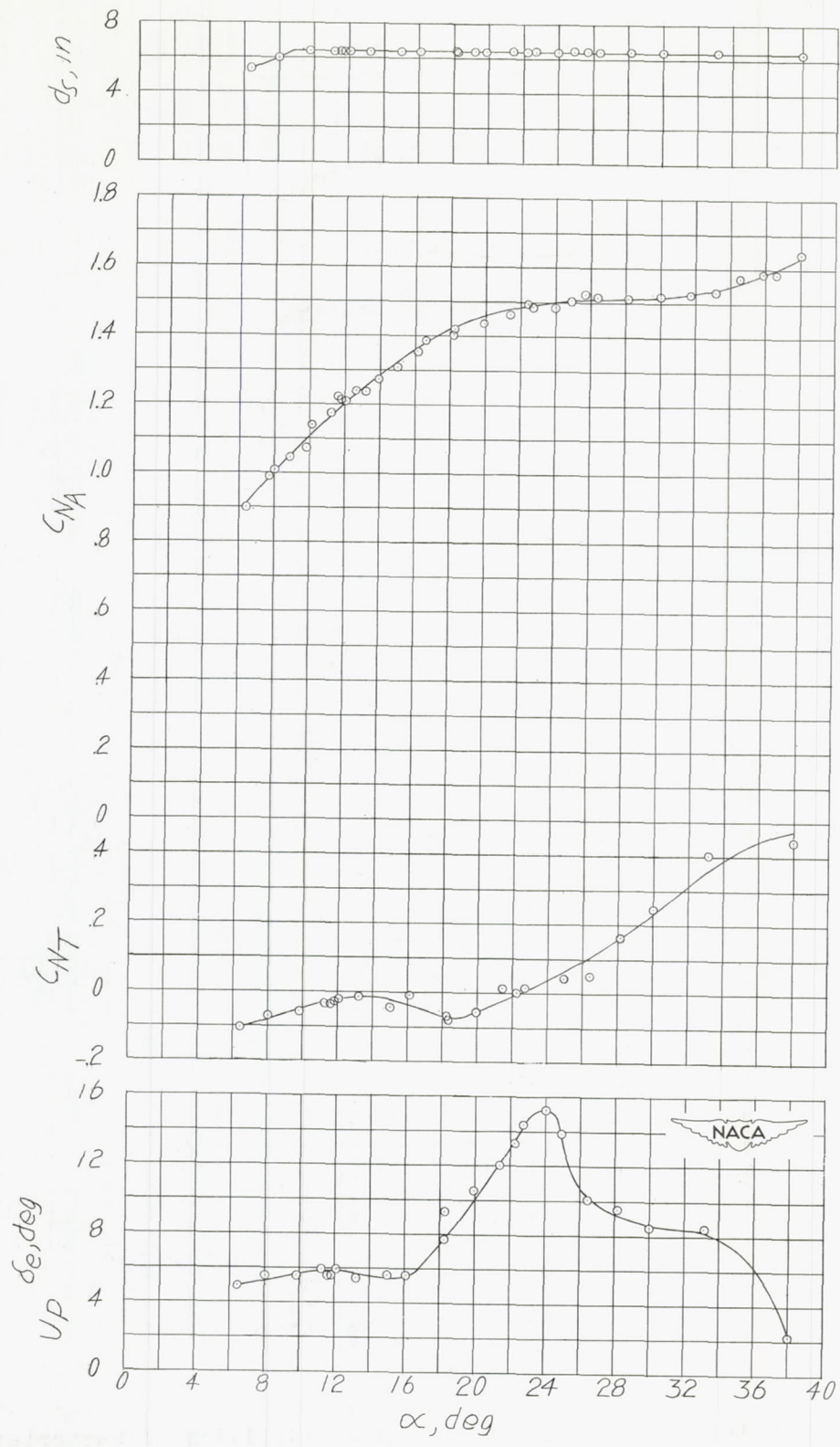
(b) δ_e , C_{NT} , and C_{NA} plotted against α .

Figure 9.- Concluded.



(a) δ_e , F_e , C_{NT} , α , and d_s plotted against V_c .

Figure 10.- Low-speed steady flight static longitudinal stability characteristics of the Douglas D-558-II (BuAero No. 37974) research airplane. Flaps down; landing gear down; slats unlocked; stabilizer setting 1.7° ; center of gravity at 26.8 percent mean aerodynamic chord.



(b) δ_e , C_{N_T} , C_{N_A} , and d_s plotted against α .

Figure 10.- Concluded.

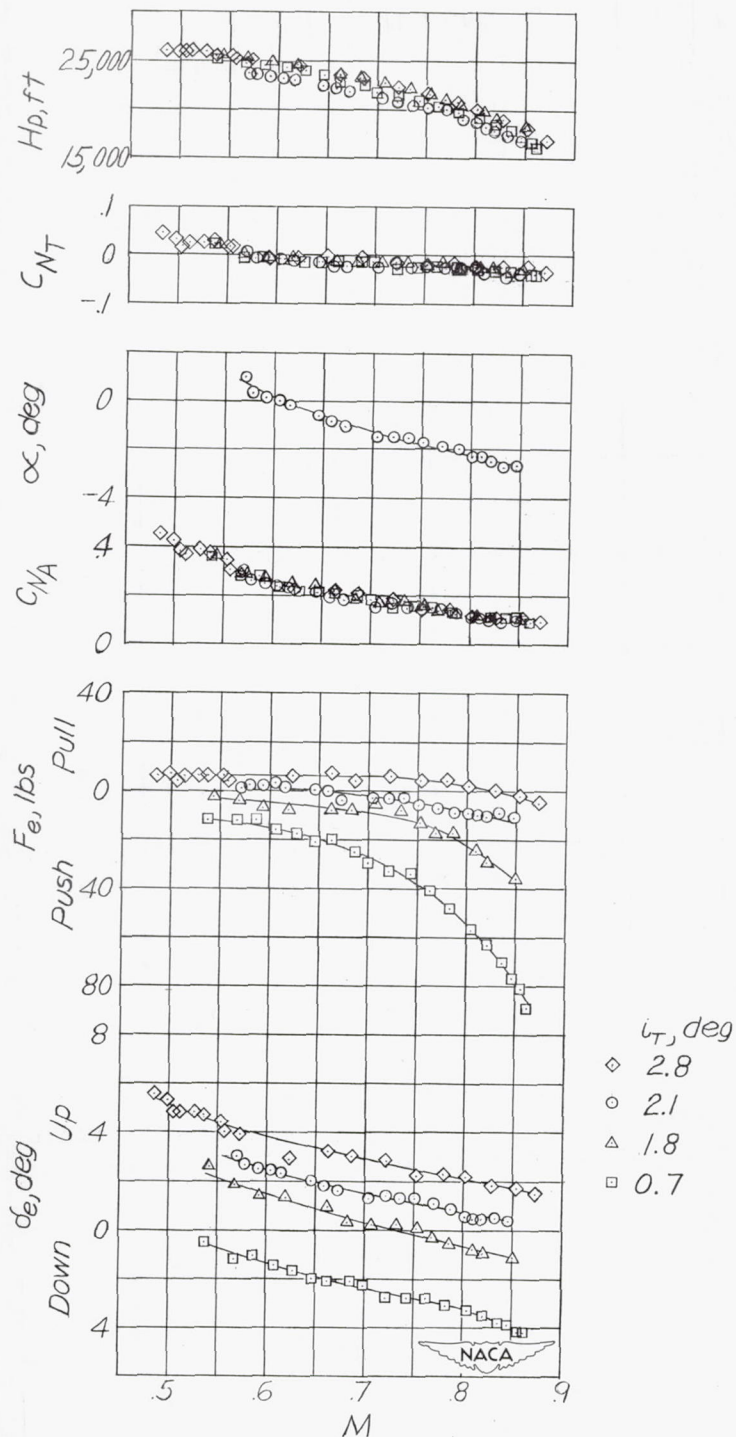


Figure 11.- Steady flight static longitudinal stability characteristics of the Douglas D-558-II (BuAero No. 37974) research airplane in the Mach number range from 0.50 to 0.87 with four stabilizer settings. Flaps up; landing gear up; slats locked; center of gravity at 26.8 percent mean aerodynamic chord.

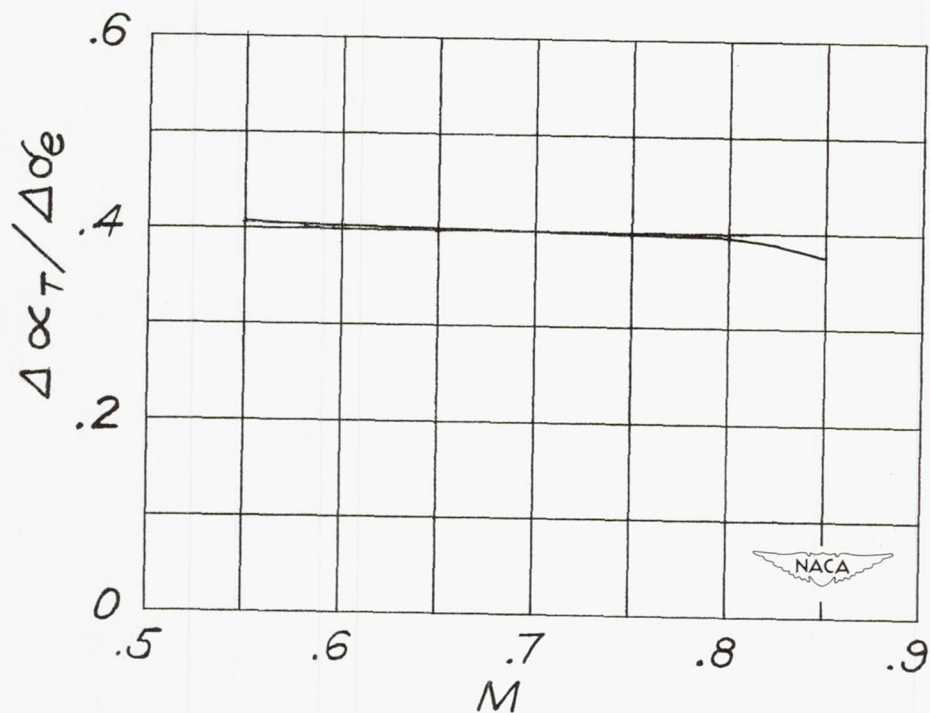


Figure 12.- Relative elevator-stabilizer effectiveness of the Douglas D-558-II (BuAero No. 37974) research airplane in the Mach number range from 0.55 to 0.85.

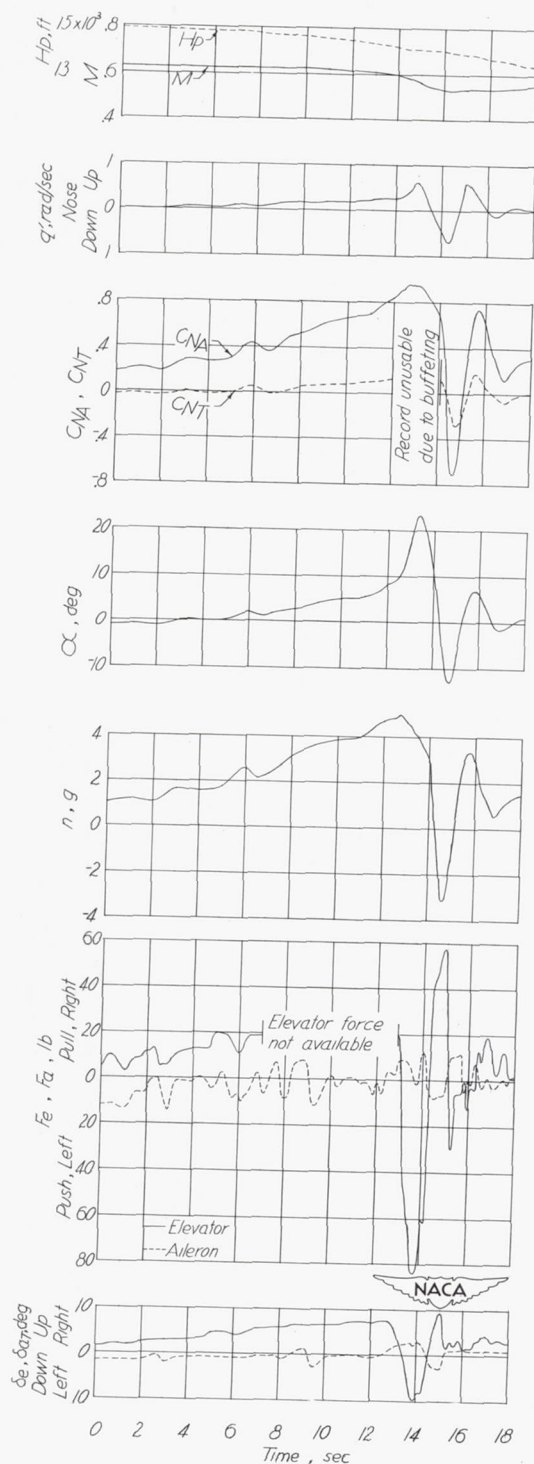


Figure 13.- Time history of a turn with the Douglas D-558-II (BuAero No. 37974) research airplane. Flaps up; landing gear up; slats locked; stabilizer setting 2.0° ; center of gravity at 27.0 percent mean aerodynamic chord.

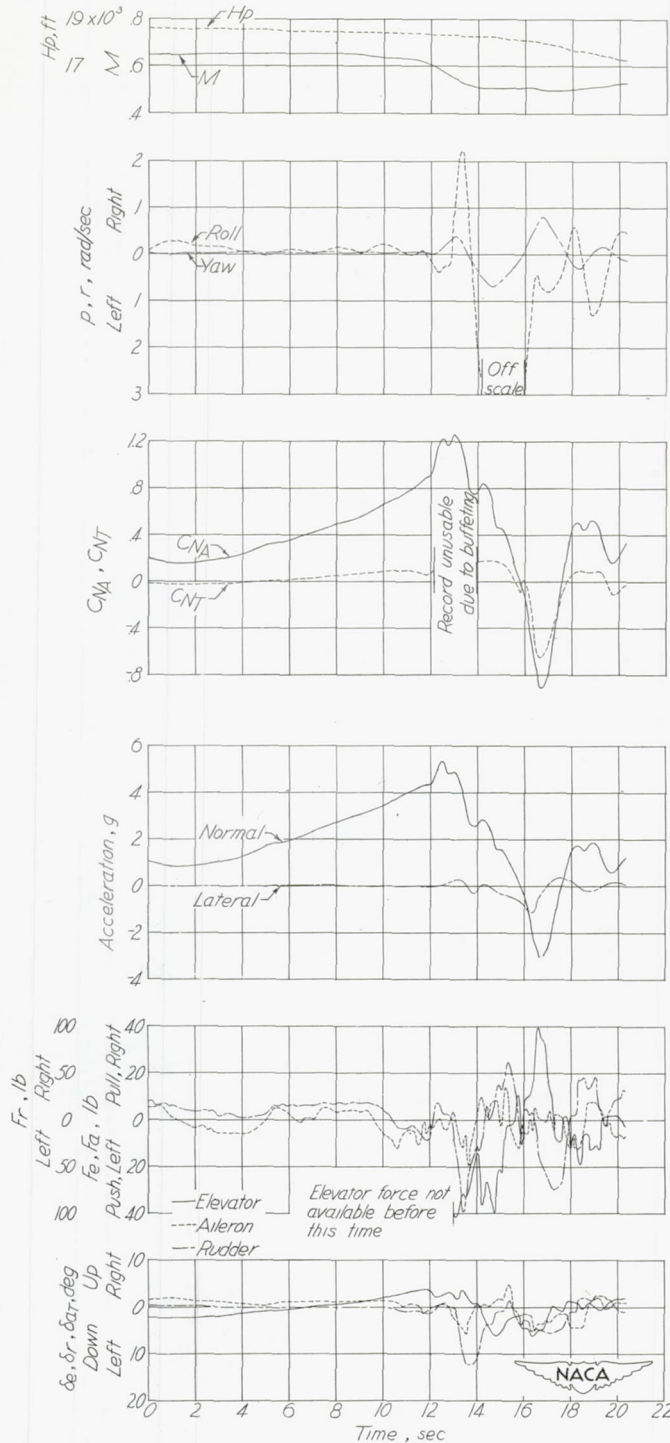


Figure 14.- Time history of a turn with the Douglas D-558-II (BuAero No. 37974) research airplane. Flaps up; landing gear up; slats locked; stabilizer setting 0.7° ; center of gravity at 26.9 percent mean aerodynamic chord.

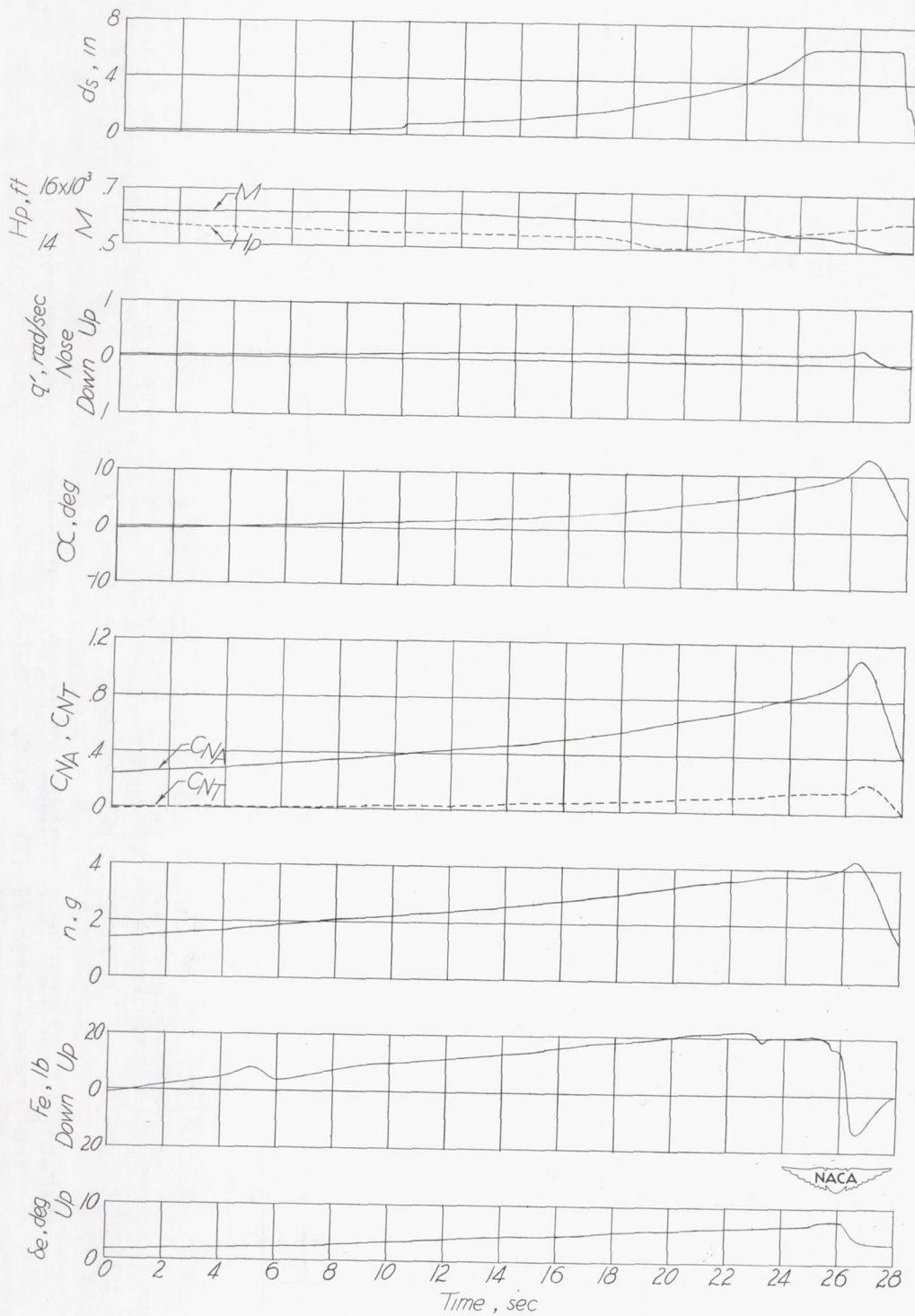
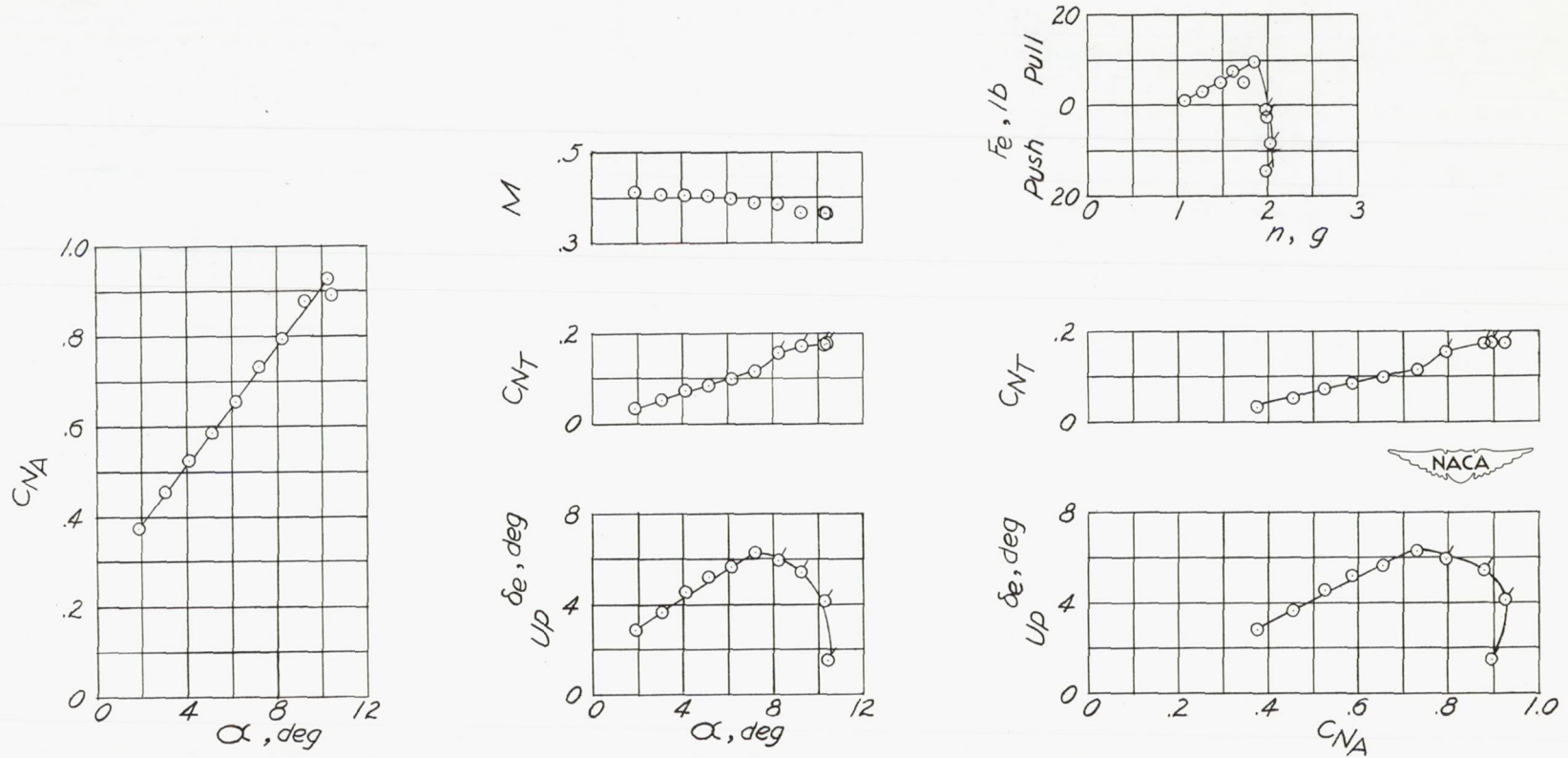


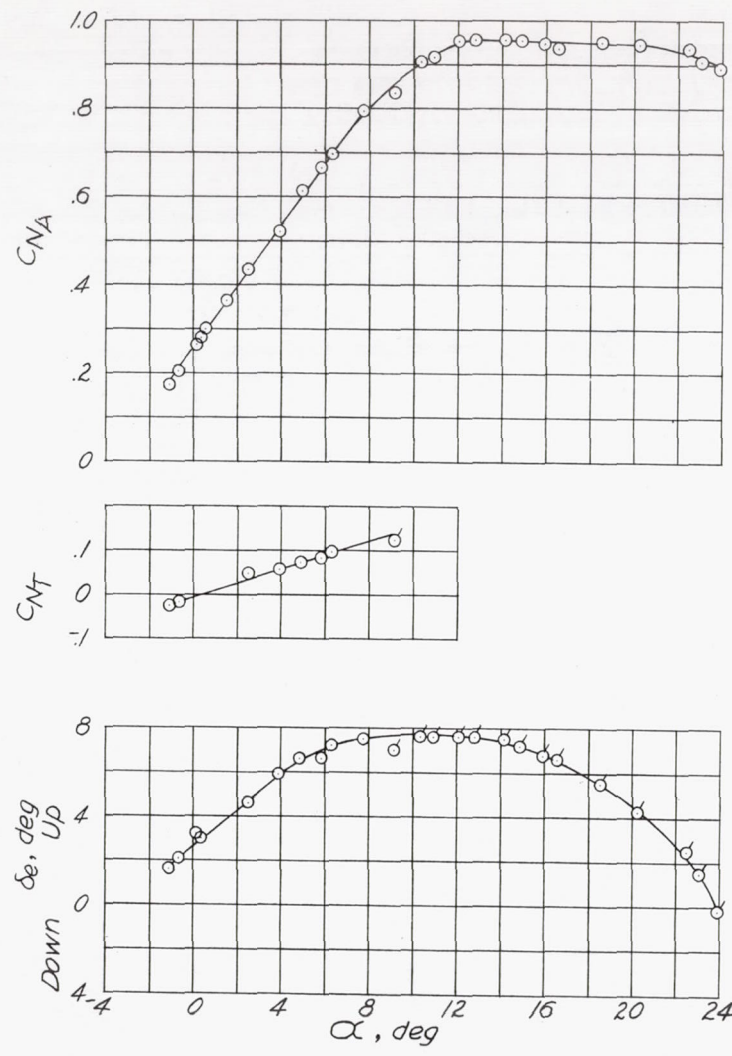
Figure 15.- Time history of a turn with the Douglas D-558-II (BuAero No. 37974) research airplane. Flaps up; landing gear up; slats unlocked; stabilizer setting 2.2° ; center of gravity at 26.7 percent mean aerodynamic chord.

o Airplane not balanced

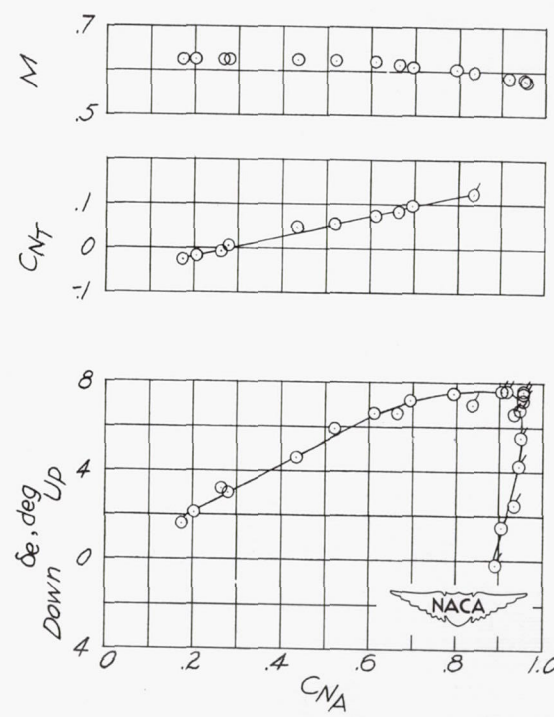


(a) $M = 0.40$; $i_T = 2.2^\circ$; center of gravity at 27.3 percent mean aerodynamic chord.

Figure 16.- Static longitudinal stability and control characteristics of the Douglas D-558-II (BuAero No. 37974) research airplane in turning flight. Flaps up; landing gear up; slats locked.



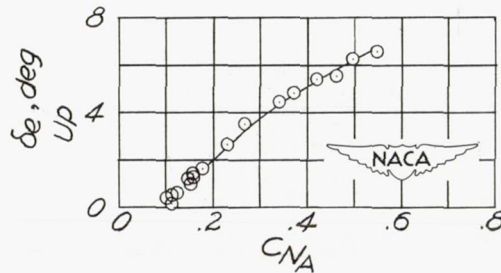
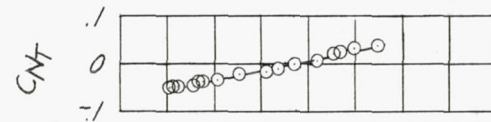
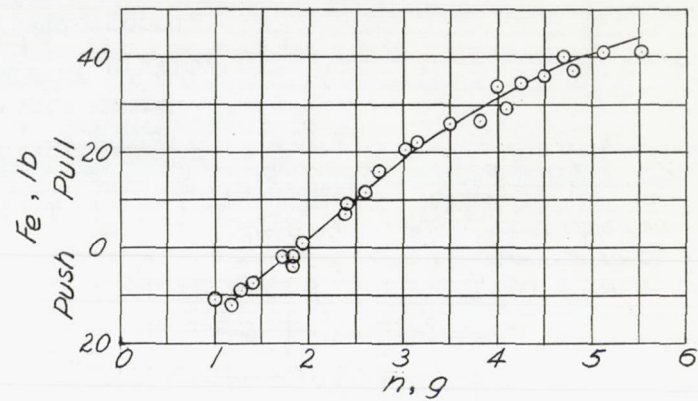
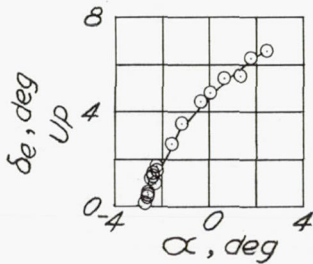
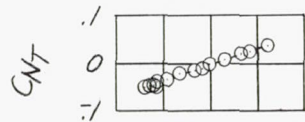
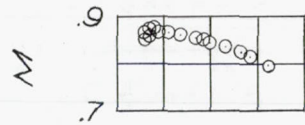
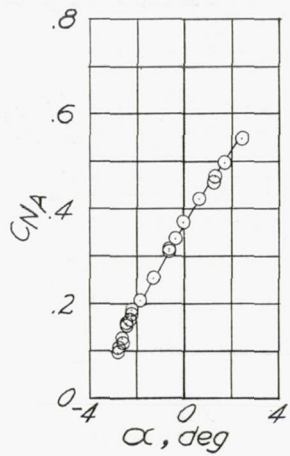
o Airplane not balanced



No elevator control force data obtained

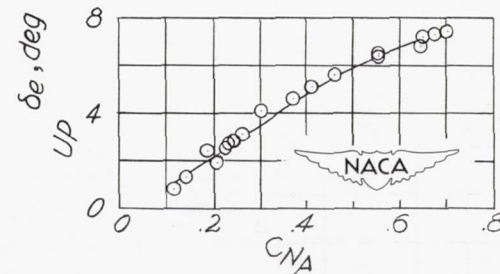
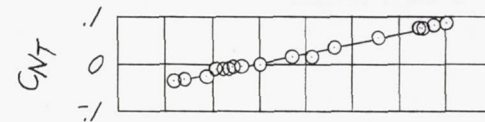
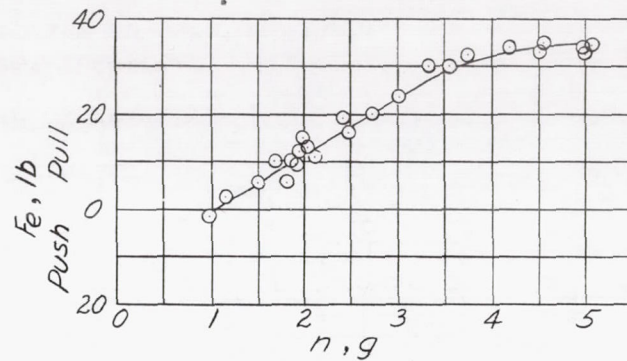
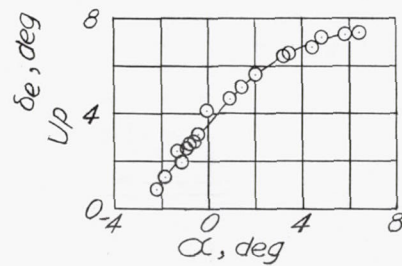
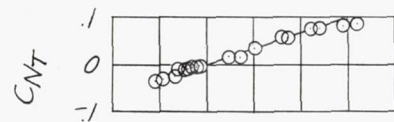
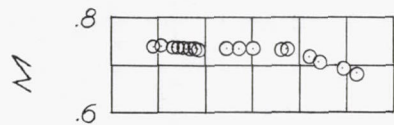
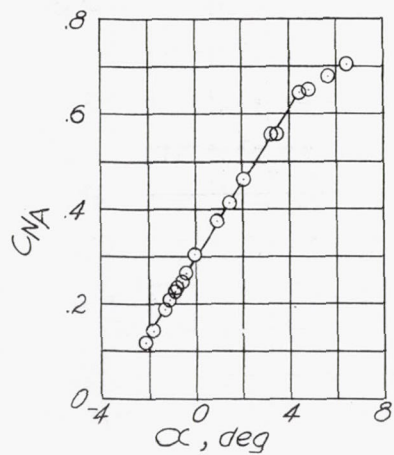
(b) $M = 0.62$; $i_T = 2.0^\circ$; center of gravity at 27.0 percent mean aerodynamic chord.

Figure 16.- Continued.



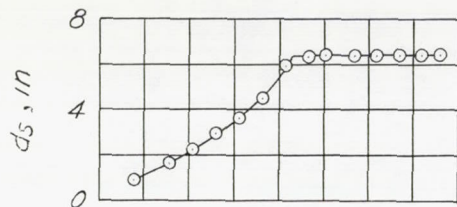
(d) $M = 0.87$; $I_T = 2.1^\circ$; center of gravity at 26.9 percent mean aerodynamic chord.

Figure 16.- Concluded.

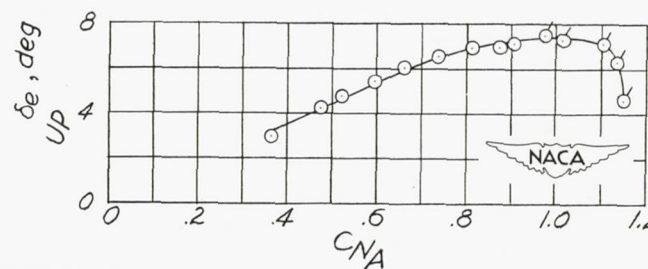
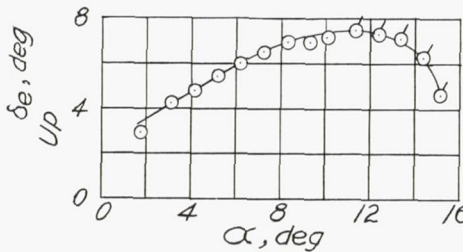
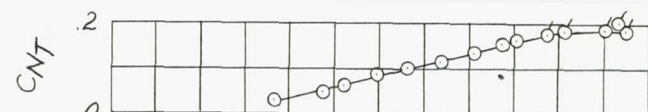
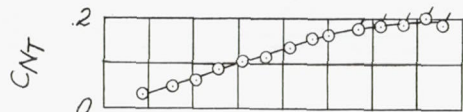
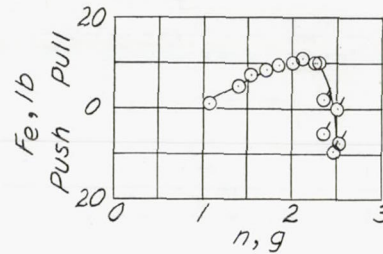
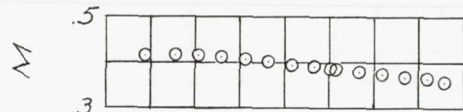
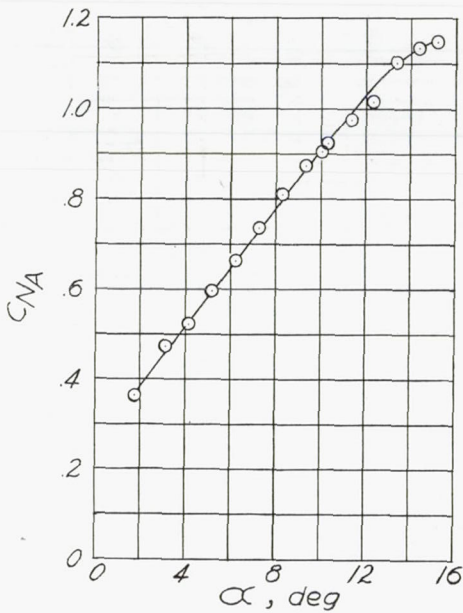


(c) $M = 0.74$; $I_T = 2.1^0$; center of gravity
at 26.9 percent mean aerodynamic chord.

Figure 16.- Continued.



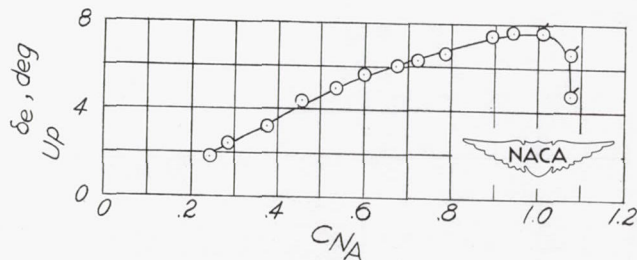
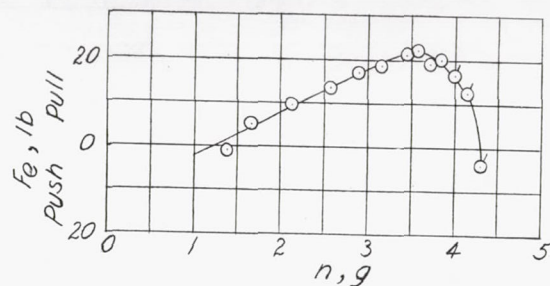
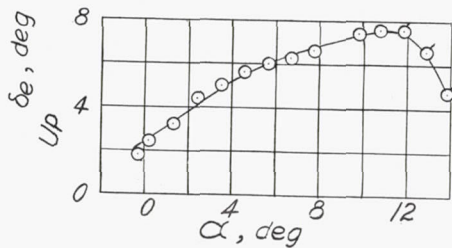
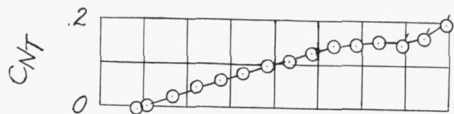
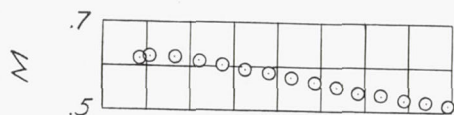
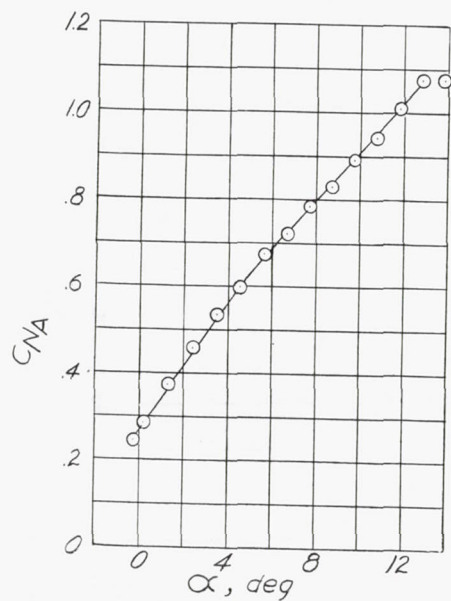
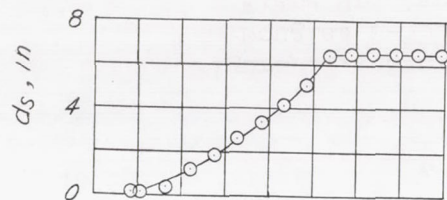
o Airplane not balanced



(a) $M = 0.40$; $i_T = 2.2^\circ$; center of gravity at 27.2 percent mean aerodynamic chord.

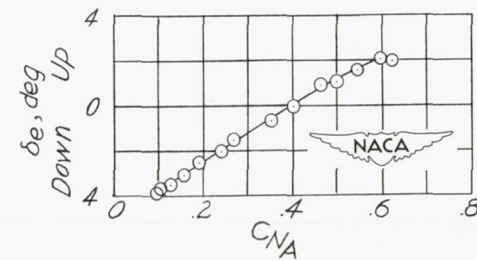
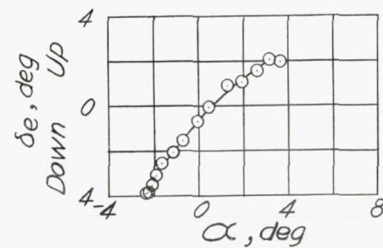
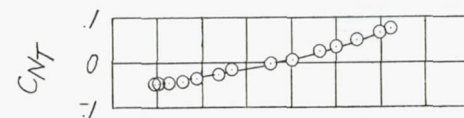
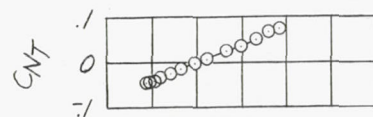
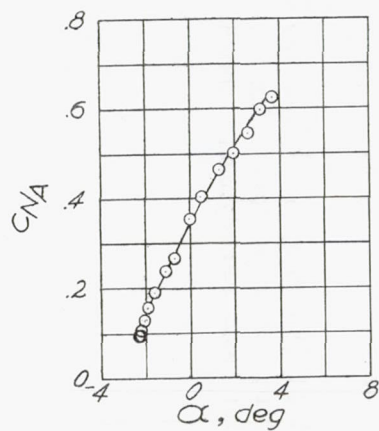
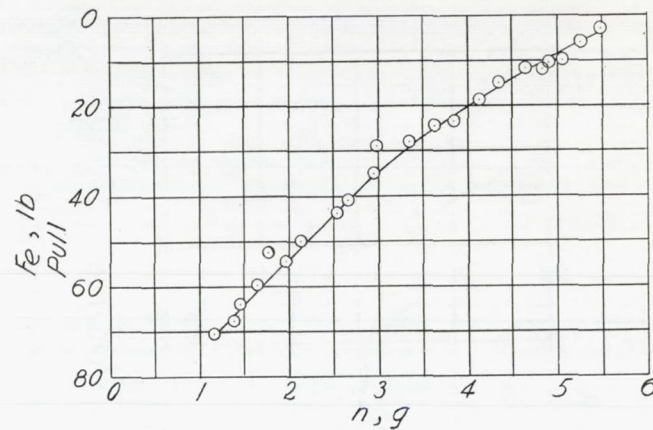
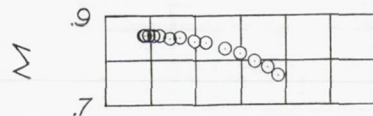
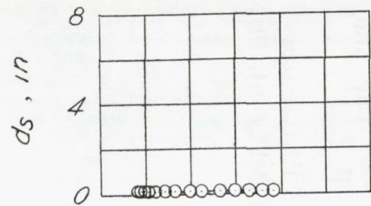
Figure 17.- Static longitudinal stability and control characteristics of the Douglas D-558-II (BuAero No. 37974) research airplane in turning flight. Flaps up; landing gear up; slats unlocked.

δ Airplane not balanced



(b) $M = 0.60$; $i_T = 2.2^\circ$; center of gravity at 26.7 percent mean aerodynamic chord.

Figure 17.- Continued.



(c) $M = 0.85$; $i_T = 0.8^\circ$; center of gravity at 27.4 percent mean aerodynamic chord.

Figure 17.- Concluded.

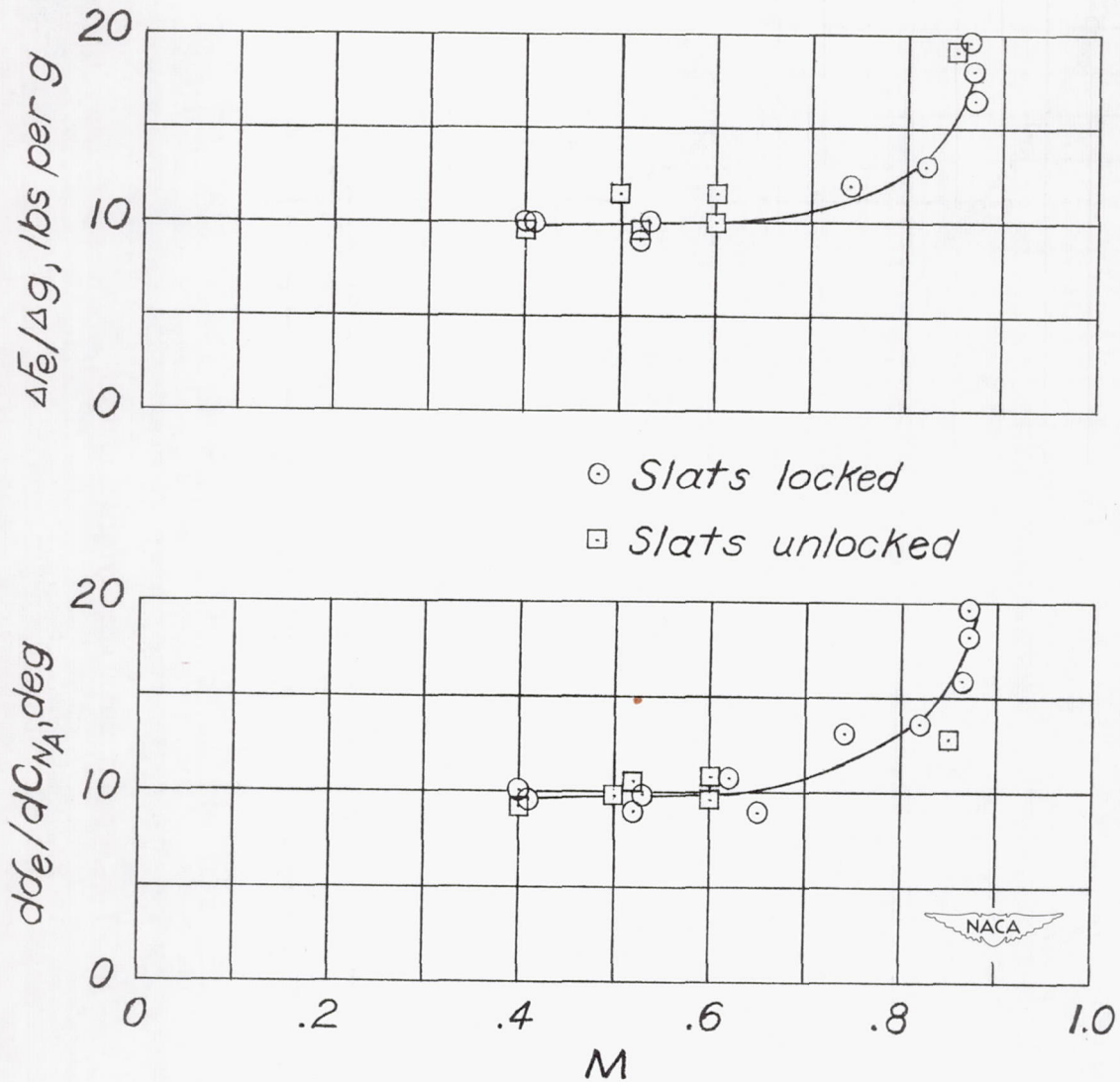


Figure 18.- The variation with Mach number of $\frac{d\delta_e}{dC_{NA}}$ and $\frac{F_e}{g}$ for the

Douglas D-558-II (BuAero No. 37974) research airplane. Flaps up; landing gear up; slats locked or unlocked; center of gravity at 26.7 to 27.4 percent mean aerodynamic chord.

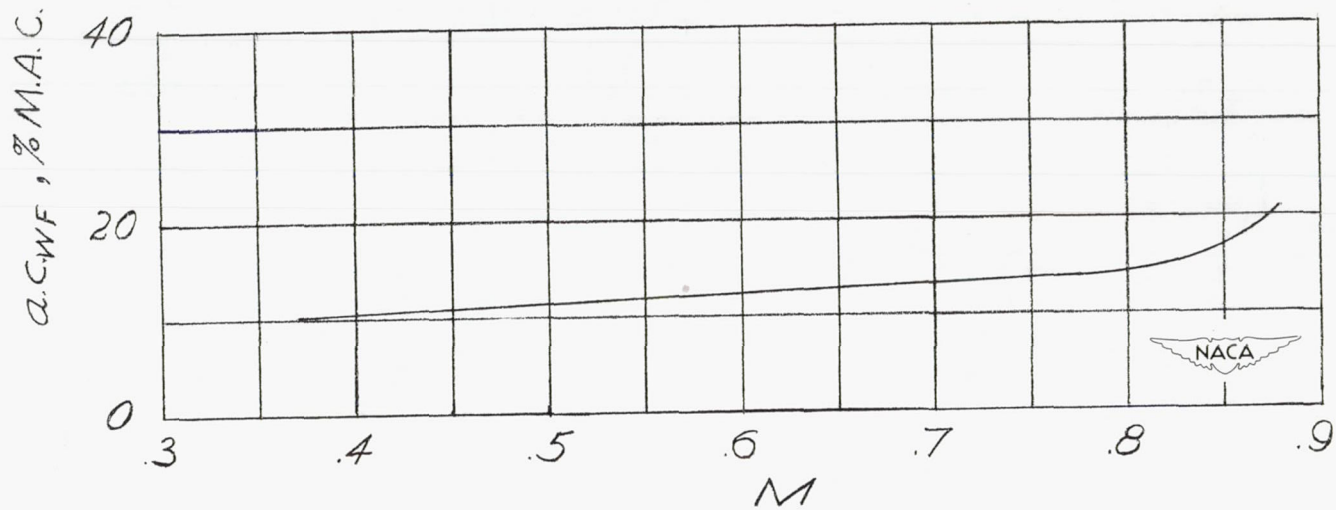


Figure 19.- The variation with Mach number of the aerodynamic-center location of the wing-fuselage combination of the Douglas D-558-II (BuAero No. 37974) research airplane. Flaps up; landing gear up; slats locked or unlocked.